NASA TECHNICAL NOTE

NASA TN D-7891

NASA TN D-7891

EVALUATION OF REFRACTORY-METAL-CLAD URANIUM NITRIDE AND URANIUM DIOXIDE FUEL PINS AFTER IRRADIATION FOR TIMES UP TO 10 450 HOURS AT 990° C

Kenneth J. Bowles and Richard E. Gluyas

Lewis Research Center
Cleveland, Ohio 44135

NATIONAL AERONAUTICS AND SPACE ADMINISTRATION • WASHINGTON, D. C. • JUNE 1975

1. Report No. NASA TN D-7891	2. Government Accession No.	3. Recipient's Catalog No.
4. Title and Subtitle EVALUATION OF REFRACTORY-METAL-CLAD URANIUM NITRIDE AND URANIUM DIOXIDE FUEL PINS AFTER IRRADIATION FOR TIMES UP TO 10 450 HOURS AT 990° C		5. Report Date June 1975 6. Performing Organization Code
7. Author(s) Kenneth J. Bowles and Richard E. Gluyas		8. Performing Organization Report No. E-7988
9. Performing Organization Name and Address Lewis Research Center National Aeronautics and Space Administration Cleveland, Ohio 44135		10. Work Unit No. 501-21 11. Contract or Grant No.
12. Sponsoring Agency Name and Address National Aeronautics and Space Administration Washington, D.C. 20546		13. Type of Report and Period Covered Technical Note 14. Sponsoring Agency Code
15. Supplementary Notes		

16. Abstract

The effects of some materials variables on the irradiation performance of fuel pins for a lithium-cooled space power reactor design concept were examined. The variables studied were UN fuel density (85 and 95 percent dense), fuel composition (UN and UO_2), and cladding alloy (Ta-8W-2Hf and Cb-1Zr). All pins were irradiated at about 990° C in a thermal neutron environment to the design fuel burnup. The 85 percent dense UN fuel (irradiated for about 10 000 hr to approximately 3 at. % burnup) gave the best overall results in meeting the operational goals. The T-111 (Ta-8W-2Hf) cladding on all specimens was embrittled, possibly by hydrogen in the case of the UN fuel and by uranium and oxygen in the case of the UO_2 fuel (irradiated for about 8300 hr to ~2 at. % burnup). Tests with Cb-1Zr cladding indicate potential use of this cladding material. The UO_2 fueled specimens met the operational goals of less than 1 percent cladding strain, but other factors make UO_2 less attractive than low density UN for the contemplated space power reactor use.

17. Key Words (Suggested by Author(s))	18. Distribution Statement
Space power reactor; Reactor materials; Irradiation: Fuel pins, T-111, Cb-1Zr, UN, UO_2; Post-irradiation examination; Capsules; Fuel; Cladding	Unclassified - unlimited STAR Category 20 (rev.)

19. Security Classif. (of this report)	20. Security Classif. (of this page)	21. No. of Pages	22. Price*
Unclassified	Unclassified	63	$4.25

* For sale by the National Technical Information Service, Springfield, Virginia 22151

CONTENTS

EVALUATION OF REFRACTORY-METAL-CLAD URANIUM NITRIDE AND URANIUM DIOXIDE FUEL PINS AFTER IRRADIATION FOR TIMES UP TO 10 450 HOURS AT 990° C

by Kenneth J. Bowles and Richard E. Gluyas

Lewis Research Cente

SUMMARY

A reference design concept for a liquid metal cooled, fast spectrum space power reactor was studied. The design goals were a life of at least 50 000 hours, a power of 2.2 megawatts (thermal), and a coolant outlet temperature of about 950° C. An in-reactor study of fuel pins incorporating selected fuel pin materials variables was conducted. It was intended that the most promising fuel-cladding combination, based on the results of this study, would be selected for further study and development. Nine fuel pins, including nominally 85 and 95 percent dense uranium mononitride (UN) and 95 percent dense uranium dioxide (UO_2) clad with tungsten-lined T-111 (Ta-8W-2Hf) and 95 percent dense UO_2 clad with tungsten-lined Cb-1Zr, were irradiated for times up to about 10 000 hours at a nominal cladding temperature of 990° C in the Oak Ridge Research Reactor (ORR). The burnup rate was accelerated to give fuel burnups expected in the reactor design concept at 50 000 hours (about 2 uranium at. % for the UO_2 fuel and about 3 uranium at. % for the UN fuel). Evaluation of the pins indicated the following:

1. Since low density (85 percent dense) UN fuel clad with tungsten-lined T-111 showed less than 0.5 percent fuel pin diametral strain under the irradiation test conditions, it shows promise of meeting the 50 000-hour life goal in the reactor concept. Fuel pins with high density (95 percent dense) UN exhibited large diametral straining (1.5 percent) of the cladding which caused rupture of the cladding.

2. The UO_2 fuel is considered to be less attractive for the fuel pin design concept because of extensive cracking of the fuel and high fission gas release (about 30 percent compared to about 4 percent for porous UN fuel). But the diametral swelling of the UO_2 fuel pins in this test was 1 percent or less.

3. The T-111 cladding embrittled and cracked at about 1.5 percent diametral strain, probably because of sensitization to hydrogen embrittlement. This is not expected to occur in an operating space reactor because of escape of hydrogen by permeation through the hot reactor vessel.

4. The Cb-1Zr appeared to be more compatible than T-111 with UO_2 fuel. Also, Cb-1Zr is less subject to hydrogen embrittlement and should be investigated as an alternate cladding material for porous UN for fuel pins limited to cladding temperatures below about 990° C.

INTRODUCTION

A reference design concept for a compact, liquid metal cooled, fast spectrum reactor for potential space power applications (termed the "Advanced Power Reactor ") was studied. The operating goal for this reference reactor was a life of at least 50 000 hours at a power level of 2.2 megawatts (thermal) and a coolant outlet temperature of 950° C. Details of the conceptual design, the materials technology program, and the nuclear design and associated critical experiments are described in references 1 to 3, respectively. The technology program, carried out in support of the design concept, was intended to determine concept feasibility, to develop long lead-time technology, and to test critical components. But before the work could be completed, the nuclear space power reactor program at the Lewis Research Center was terminated. Although incomplete, some parts of the program had progressed to the point where useful information was obtained. The status of the overall program at its close and the results of the materials technology efforts are summarized in reference 4.

The fuel pins for the proposed reactor concept consisted of uranium mononitride (UN) cylinders clad with tungsten-lined T-111 (Ta-8W-2Hf) as shown in figure 1 (also see ref. 1). Under operating conditions the cladding of the fuel pins would be subjected to stresses from fission gases released from the fuel, and from fuel swelling caused by the accumulation of gaseous and solid fission products in the fuel; damage by neutron bombardment; and possible reactions involving fuel-cladding, cladding-coolant, and cladding-fission products. Also, fuel-coolant reactions might be a problem in case of a defect in the cladding. To compensate for these possibilities for fuel pin degradation, the limit for maximum fuel pin diametral strain was established at 1 percent in 50 000 hours and preferably the cladding should remain ductile and free from cracks. In addition, the fuel must be maintained in a stable configuration within the core of the reactor to assure adequate reactor control.

This report presents the results of one part of an in-reactor fuel pin irradiation study conducted in support of the design concept. The other parts of the fuels irradiation program are presented in references 5 to 7. The prime emphasis of these studies was for evaluation of the irradiation performance of 95 percent dense UN clad with T-111.

The part of the study described in this report was primarily an investigation of the effects selected materials variables had on fuel pin performance under irradiation. The main emphasis was on the prime fuel pin materials UN and T-111 but the uranium dioxide (UO_2) fuel and a columbium alloy cladding (Cb-1Zr) were included as possible alternate materials. Unpublished calculations for a UO_2 fueled reactor design, equivalent to the UN fueled reference reactor design, indicate a need for a larger reactor with a higher uranium atom inventory for the UO_2 fueled reactor than for the UN fueled reactor. This results in a smaller end of life burnup for the UO_2 fuel (~2 at. %) than for the UN fuel (~3 at. %).

The specific objectives of the fuel pin irradiation tests carried out in this experiment were as follows:

(1) To compare the irradiation performance of low density (~85 percent dense) UN containing interconnected porosity with that of high density (~95 percent dense) UN with enclosed porosity in fuel pins clad with T-111 (Ta-8W-2Hf)[1]

(2) To compare the irradiation performance of a UO_2 fuel pin clad with T-111 to the performance of UN fuel pins clad with T-111

(3) To compare the irradiation performance of UO_2 fuel pins clad with T-111 to the performance of UO_2 fuel pins clad with Cb-1Zr[1]

(4) To select the most promising fuel-cladding combinations for further development and to identify potential problems

This experiment involved the design, fabrication, and irradiation of nine fuel pins (0.953 cm (3/8 in.) diam by 11.43 cm ($4\frac{1}{2}$ in.) length). Most of the study was done at the Oak Ridge National Laboratory (ORNL) under a NASA-funded interagency agreement with the Atomic Energy Commission. Under this agreement the ORNL constructed and irradiated the fuel pins and their containment capsules, disassembled the capsules after irradiation, and did a preliminary external examination of the fuel pins (ref. 8). The pins were irradiated in the Oak Ridge reactor at approximately 990° C for times up to about 10 000 hours. For comparison, eight other fuel pins, each identical to one of the irradiated fuel pins, were tested out of pile in an ultrahigh vacuum system at similar temperature and time conditions. A few selected fuel pins and the corresponding thermal simulation pins were sectioned and examined at Lewis. This report summarizes the results of the entire experiment with major emphasis on the results of the postirradiation examination on the selected pins.

Irradiation tests of UN fuel pins have been conducted at other laboratories (refs. 9 to 13). Most of these investigations, however, were carried out at higher temperatures (1100° C to 1450° C) than the prime fuel pin cladding temperature (~990° C) of interest for this reactor concept. Cladding materials were mainly columbium and tungsten alloys, and the fuel was limited to high density UN (95 percent dense). Thus, a direct comparison of the behavior of UN and UO_2 was not made under the conditions of interest here.

[1]All fuel pin claddings (both T-111 and Cb-1Zr) used in this experiment were lined with thin tungsten foil to minimize any fuel-cladding reactions.

REVIEW OF CAPSULE DESIGN, FABRICATION, AND IRRADIATION AND THERMAL CONTROL HISTORY

The capsule and fuel pin design, fabrication, and irradiation (as well as preparation and aging of thermal control specimens) were carried out at ORNL. These areas are summarized in the following sections. A more detailed treatment can be found in references 8 and 14.

Fabrication of Fuel Pins

Eleven UN fueled and six UO_2 fueled test pins were fabricated. Six of the UN and three of the UO_2 pins were used for irradiation testing and five UN and three UO_2 pins were used for out-of-reactor thermal testing. Descriptions of all the fuel pins, including pretest dimensions, weights of fuel pins components, densities of the fuel pellets, and fuel enrichments, are tabulated in tables I and II. For simplicity, subsequent discussions of the fuels will refer to the fuel in pins 12 and 14 as 95 percent dense UN, to the fuel in pins 10, 11, 13, and 15 as 85 percent dense UN, and to the fuel in pins 16, 17, and 18 as 95 percent dense UO_2. All of the test pins were similar in configuration. A sketch of a typical test pin is shown in figure 2.

As shown in figure 2, eight to ten fuel pellets are contained within each fuel pin. The fuel was separated from the cladding and end caps by the tungsten liner and two cylindrical tungsten spacers. This separation of fuel and cladding materials was necessary to prevent fuel-cladding reactions (ref. 15). The hemispherical T-111 washers were used to help position the fuel axially within the fuel pin. These washers were intended to deform during irradiation testing to accommodate thermal expansion and irradiation-induced swelling of the fuel in the axial direction without transferring unnecessarily large stresses to the cladding.

Fabrication and assembly of the fuel pins, irradiation capsules, and thermocouples used quality assurance procedures developed as a part of this irradiation program. The details of the quality assurance procedures are presented in reference 8.

Characterizations of all materials were carried out as an integral part of the fabrication and assembly procedures. Chemical analyses of the fuel materials are presented in tables III and IV. The cladding materials were purchased under the materials specifications presented in reference 16.

The cladding and end plugs of the fuel pins were fabricated from tubing and rod, respectively. All fuel pins were lined with a free standing cylindrical tungsten liner. The liner was formed by hot isostatically pressing five layers of 0.0025-centimeter (0.001-in.) tungsten foil over a molybdenum mandrel inside a sealed molybdenum can. The

layers of foil were bonded together under a pressure of 2.1×10^8 newtons per square meter (30 000 psi) at 1665° C for 1 hour. After pressing, the outer can was stripped away by chemical dissolution and the liner outside diameter was ground to size. The final fabrication step was the removal of the molybdenum mandrel with acid (10 percent H_2SO_4, 40 percent HNO_3, and 50 percent H_2O by volume).

The 95 percent dense UN and UO_2 cylinders were fabricated with an axial hole along the centerline. The 85 percent dense UN cylinders had no axial hole so that the pins containing this fuel had the same "smear" density of fuel as the pins containing high density fuel. (The "smear" density of the fuel is obtained by dividing the total weight of fuel by the volume enclosed by the cladding over the length of the fuel stack.) The length of the fuel stack was the same for all of the fuel pins.

The fabrication procedures for the UN fuel are described in reference 17. It should be pointed out that the uniaxial dry pressing technique used in this study produced pellets which were apt to contain small circumferential cracks. The UO_2 fuel was fabricated by similar techniques. However, there was a difference in the preparation of the powder from which the pellets were pressed. The UN powder was made by a hydride-dehydride-nitride process from uranium metal appropriately enriched in U-235. The UO_2 powder, on the other hand, was obtained by blending UO_2 powder depleted in U-235 with 93 percent enriched UO_2 powder in the required ratios to produce the final enrichment desired.

The fuel pins were assembled using the procedures outlined in appendix A. A typical as-fabricated fuel pin is shown in figure 3.

Capsule Design and Assembly

The fuel pins were irradiated in three capsule assemblies which each contained three fuel pins stacked end to end. Two of the capsule assemblies (identified as UN-4 and UN-5) contained the six fuel pins using the UN fuel. The other capsule assembly (UN-6) contained the three fuel pins with the UO_2 fuel (see table I). The capsules were designed to produce the desired fuel pin cladding temperature (990° C), and they were instrumented to allow the determination of both the cladding temperature and the heat flow from the fuel to the reactor coolant water. The heat flux was used to calculate burn-up as the testing proceeded (ref. 14).

The three fuel pins in each capsule were positioned as shown in figure 4. Chromel-Alumel thermocouples are positioned in the NaK-76 filled gap and also along the secondary containment vessel. The thermocouples on the secondary containment vessel are positioned in pairs, one on the outside surface and one inside the vessel wall to measure the temperature drop through the wall. Details of the capsule design, thermocouple positions, and assembly are given in references 8 and 14.

Capsule Irradiation

Each capsule was suspended in position at the reactor face by a stainless steel support tube which served as a lead tube to conduct the thermocouple leads and gas lines from the capsule to the instrumentation leads at the side of the Oak Ridge reactor pool. The capsule itself could be moved toward or away from the face of the reactor to vary the neutron flux level. The estimated thermal neutron flux level along the fuel column was 1.2×10^{13} to 1.5×10^{13} neutrons per square centimeter per second. The axial flux profile along the capsule was such that the top fuel pin in each capsule was exposed to a lower flux than the other two fuel pins. The heat generation rates in these top pins were the same as those in the other two pins because the U-235 enrichment was increased appropriately. Since the T-111 cladding in the middle UO_2 fueled pin (pin 17) afforded more neutron shielding than the Cb-1Zr cladding, the fuel in pin 17 also contained a higher enrichment of U-235. The thermal fluence received by the fuel during irradiation was 4.3×10^{20} to 8.6×10^{20} neutrons per square centimeter for the UN fuel (~10 000 hr) and 3.4×10^{20} to 6.9×10^{20} neutrons per square centimeter for the UO_2 fuel (~8000 hr).

The effective fast neutron flux ($E \geq 1$ MeV) was one order of magnitude lower than the effective thermal flux or about 1.2×10^{12} to 1.5×10^{12} neutrons per square centimeter per second. The fast neutron flux of the reference space power reactor concept is calculated to be 3.5×10^{13} neutrons per square centimeter per second (for energies $\geq$ 0.82 eV) (ref. 1). This is over an order of magnitude greater than that experienced by the materials in this test program. Therefore, the testing in the thermal flux of the Oak Ridge reactor did not generate information on the effects of fast neutrons (at fluences of about 10^{22} neutrons/cm^3) on the swelling, ductility, and creep properties of the cladding at high temperatures.

The two capsules containing the UN fueled pins were designed to operate with a heat generation rate of 28.2 to 30.2 kilowatts per meter (8.6 to 9.2 kW/ft) to maintain the cladding temperature at about 990° C with a ΔT of about 125° C across the radius of the fuel. The actual heat generation rate, calculated from the calorimeter measurements during irradiation, was found to be 31.2 to 36.1 kilowatts per meter (9.5 to 11.0 kW/ft).

Difficulties were encountered in operating the capsule containing UO_2 fuel pins at design conditions. Because the thermal conductivity of UO_2 is less than that of UN, an additional requirement of this capsule design was to limit the fuel pellet centerline temperature to $<1600^\circ$ C. This limit was selected to minimize fuel redistribution and/or fuel restructuring of the UO_2 during irradiation. Calculations predicted that a heat generation rate of 19.7 kilowatts per meter (6 kW/ft) would maintain the cladding at 990° C and the fuel centerline at about 1550° C. However, on insertion of the capsule for irradiation it was found from cladding and calorimeter temperature measurements that higher centerline temperatures would result from operation at a cladding temperature of 990° C. Therefore, the fuel pins were held at a reduced power of 13.4 to 16.7 kilowatts

per meter (4.1 to 5.1 kW/ft) for the first 1500 hours of irradiation while methods for achieving experiment design conditions were investigated. During this period the cladding temperatures were 880° C and the fuel centerline temperatures were about 1500° C. It was found that the design conditions could be met by replacing the helium in the outer gas-filled conduction gap (see fig. 4) with argon and using a heat generation rate lower than 19.7 kilowatts per meter (6.0 kW/ft). Therefore, this change was made and the pins were operated at the design cladding temperature (990° C) for the remainder of the test.

Reactor cycles were 6 weeks in duration with two short refueling shutdowns during each cycle. Thus, in about every 900 hours of fuel pin irradiation the fuel pins experienced three thermal cycles between 990° and 120° C. The UN fueled pins experienced a total of 34 or 35 thermal cycles while the UO_2 fueled pins experienced 28 thermal cycles.

Temperature Measurements

During the course of the irradiation tests the failure rate of the Chromel-Alumel thermocouples in the NaK was high. More than half of the NaK-exposed thermocouples used in this experiment failed. These failures apparently were due to the formation of a parasitic junction in a cool zone of the thermocouple lead (see ref. 8).

Early in the testing a reliable relationship was established between the heat generation rate, as calculated from the thermocouples on the outer Zircaloy 2 containers, and the cladding temperatures. So, in spite of the high rate of failure of the NaK-exposed thermocouples, operation of the capsules was maintained in a reliable manner with those NaK thermocouples which continued to function satisfactorily and with the calculated heat generation rates.

The fuel pin temperature variations as a function of position and time were quite complex and are discussed in more detail in reference 8. As mentioned earlier, each pin was instrumented with two cladding thermocouples. The junctions of these thermocouples were placed opposite each other at the axial midplane of the pin. One of the two thermocouples on the middle pin of each capsule was used as the control couple except where the thermocouple failure necessitated a shift to a thermocouple on another pin. The middle control pin in each capsule could be held within ±15° C of the target temperature by adjusting the distance of the capsule from the face of the reactor to compensate for changes in flux level during a reactor cycle. Under these conditions the top and bottom fuel pin experienced a measured temperature variation of ±50° C during a cycle. The time-averaged axial midplane temperatures of all of the pins were within the 925° to 1010° C range in this experiment. The maximum measured circumferential temperature difference for a pin was about 20° C. The axial cladding temperature gradients the pins were not measured but were estimated by heat transfer calculations. The average axial

temperature in the central 3.8-centimeter (1.5-in.) section of the fuel pin cladding decreased about 20° C per centimeter from the axial midplane of the pins. At the ends of the fuel column, the calculated temperature fell to as low as 700° C. (The fuel and cladding specimens used for postirradiation evaluation were taken from the central portions of the fuel pins.)

Fission Gas Monitoring

At the end of every 6-week reactor cycle, the cover gas over the NaK in each capsule was sampled to monitor for fission gases. Detecting any fission gases could incicate cladding ruptures or leaking fuel pins.

Fission gases were initially detected in capsule UN-4 at the end of the first reactor shutdown. The measured activity level was very low and appeared to remain constant throughout the rest of the irradiation test. Traces of fission gases were first detected in capsule UN-5 after 8500 hours of continued irradiation. No fission gases were detected in capsule UN-6 at any time during the irradiation test. Approximate calculations, based on the free volume of the capsule and the level of activity of the gas samples, indicated a very small amount of fission gas was released from the fuel pins in capsules UN-4 and UN-5 (less than 0.01 percent of the fission gas expected to be released from the UN fuel). This low amount suggested leakage through a very small cladding crack or pore.

Neutron Radiography

Neutron radiography facilities at ORNL (see ref. 19) were used to observe the condition of the fuel pins during irradiation. Observations of primary interest were fuel swelling, cladding diametral changes, and integrity of fuel and cladding (i.e., areas of reaction or crack development).

Each capsule was radiographed three times: (1) before the irradiation test, (2) sometime after half of the irradiation time had elapsed, and (3) after irradiation was completed. Each time the capsule was radiographed from three angles: 0°, 45°, and 90°. (The 0° angle was of the side of the capsule nearest to the reactor during irradiation.)

Cladding cracks and fuel cracks were observed in some cases. But a quantitative measurement of changes could not be made because of (1) the lack of clear fuel pin edge delineation because of thermocouple interference, (2) flux gradients, both axial and radial, and (3) the unsharpness effect from both the film and the radiograph camera which

resulted in inconsistent measurements. These problems are discussed in more detail in reference 20.

Qualitative information obtained from the neutron radiographs is summarized as follows:

(1) No cracks were observed in the cladding of fuel pin 12 (95 percent dense UN clad with T-111) after 7200 hours or irradiation. But a major cladding crack was observed in this pin after 10 450 hours of irradiation.

(2) A major cladding crack was observed in fuel pin 14 (95 percent dense UN clad with T-111) after 9000 hours of irradiation.

(3) Fuel cracking was first observed in the midtest (after 6000 hr) examination of the UO_2 pins and in final examination (after 10 450 hr) of the pins containing 95 percent dense UN. Neutron radiography on completion of irradiation indicated more extensive cracking of UO_2 pellets than of UN pellets. Fuel cracking was mostly transverse in the UO_2 pellets and longitudinal in the UN pellets.

Out-of-Reactor Thermal Controls

Six weeks after the irradiation of a pin was started, an identical unirradiated pin was placed in a high vacuum (1.3×10^{-7} N/m^2 (10^{-9} torr)) furnace and subjected to a thermal history approximating that of the irradiated pin. The thermal conditions of these tests differed in some respects from those experienced by the irradiated fuel pins. Because the fissioning process produces heat internally in the fuel, a temperature drop of about 125° C exists across the radius of the irradiated fuel pellet. This was not reproduced in the out-of-reactor thermal testing in which heat was supplied by external radiation heaters. Also, the irradiated fuel pin was exposed to a NaK environment rather than to the vacuum environment of the thermal simulation pin. And the cooling rate of the thermal simulation pin was slower than that of the fuel pin in the reactor during shutdown. These tests, however, are believed to adequately simulate the potential effects of any cladding aging effects, cladding-liner reaction, liner-fuel reactions, or of any reactions between the cladding and products originating from thermal decomposition of fuel.

Capsule Disassembly

After the capsule irradiation and neutron radiography were completed, the three capsules were transferred to the Oak Ridge reactor hot cells. The lead tubes were sheared about 15 centimeters (6 in.) above the top stainless steel thermocouple feedthrough. All gas lines and thermocouples were crimped and sealed with epoxy cement. The capsules then were transported to the Oak Ridge High Intensity Radiation Level

Examination Laboratory for further disassembly and nondestructive examination of the fuel pins.

The two outer containment vessels (Zircaloy and stainless steel) were removed without cutting the thermocouples or the gas lines. This left the NaK containment vessel (Cb-1Zr) intact for a visual inspection for leaks or other gross changes (e.g., deformation, oxidation, or corrosion) which could have affected the operating characteristics of the capsule during the irradiation tests. The NaK containment vessels were then photographed, and diametral measurements were made using opposing dial gages. No unusual changes were noted.

The containment vessels were emptied of NaK by cutting off the bottom of each vessel and blowing the NaK out with purified argon. Then the vessels were immersed in mercury to remove the remaining NaK by amalgamation. Mercury was used rather than anhydrous liquid ammonium or an alcohol for removing the NaK to minimize the risk of hydrogen embrittlement of the T-111 (ref. 21). After two washings in clean mercury the top of each vessel was cut off and the fuel pins were removed and immersed in mercury. After the fuel pins were removed from the last wash of mercury, they were found to be coated with a very light white film which was assumed to be oxides of potassium and/or sodium. The pins which had no visible cracks were rinsed with distilled water to remove this film and then immediately dried. Photographs of representative posttest fuel pins are shown in figure 5.

The T-111 positioning extension at the lower end cap of each of the three pins in capsule UN-4 were broken off during removal from the NaK containment vessel. Because of the care taken in NaK removal, this was taken as evidence that the T-111 cladding was brittle in the as-irradiated condition.

FUEL PIN EVALUATION

While the preliminary examination of the irradiated fuel pins was performed at ORNL, the more detailed evaluation was done at the NASA Plum Brook Reactor Facility Hot Laboratory. The evaluation included the following:

(1) Visual examination
(2) Measurement of cladding diameter and fuel pin weight
(3) Helium mass spectrometer leak checks
(4) Fission gas measurement and analysis
(5) Axial gamma scanning for fuel burnup profile
(6) Fuel burnup by isotopic measurement
(7) Measurement of fuel cylinder diameter
(8) Cladding ductility measurements
(9) Fuel density measurements

(10) Visual observations such as liner cracks, fuel redistribution, and appearance of end spacers

(11) Metallography of fuel and cladding

The pins were leak checked, weighed, and dimensionally measured. However, the other tests were performed only on selected specimens. One representative fuel pin from each of the four fuel-cladding combinations tested was selected for this evaluation. These were as follows:

Fuel pin 11: T-111 and 85 percent dense UN

Fuel pin 14: T-111 and 95 percent dense UN

Fuel pin 17: T-111 and 95 percent dense UO_2

Fuel pin 18: Cb-1Zr and 95 percent dense UO_2

The corresponding thermal control pins were evaluated similarly. The remaining fuel pins were shipped to ORNL for storage in the event that there is interest in evaluating these at some later time. The following sections summarize the general procedures used in these evaluations and the results obtained.

Fuel Pin Weight and Dimensional Measurement

Each fuel pin was examined visually for possible damage from shipping and then weighed to a precision of ±5 milligrams. These weights, adjusted to include the calculated weights of the broken extensions, are compared to the preirradiation weights in table V. The weight changes are considered negligible except for pins 12 and 14 which confirm the penetration of the cladding by NaK.

Preirradiation dimensional measurements of the fuel pins were made with precision micrometers. The results are presented in appendix B. Postirradiation measurements were made with a profilometer consisting of opposing dial gages calibrated with a 0.9538-centimeter- (0.3755-in.-) diameter stainless steel standard cylinder. These measurements were checked with an optical gage. The measurements of the fuel pin diameters were made at 1.27-centimeter (0.5-in.) intervals along the longitudinal axis starting 1.27 centimeters (0.5 in.) from the top end. Measurements were made at 0° and 90° orientations. (The 0° orientation corresponds to the side of the pin closest to the reactor face.)

The diameter changes are shown in figure 6. Except for the two pins which were ruptured (pins 12 and 14), the diameter changes were less than the 1 percent strain goal established for this fuel pin design. Since the profilometer measurements could be plotted to show the fuel pin cladding wall profiles (diametrically opposite each other), measurements of radial cladding changes on the wall of a cracked fuel pin directly opposite the crack could give an estimate of the amount of cladding strain present when the

crack occurred. These measurements were made, and it was estimated that fuel pin 14 cracked at about 1.5 percent diametral strain.

Helium Mass Spectrometer Leak Tests

All of the fuel pins, except for pins 12 and 14 (both of which were 95 percent dense UN clad with T-111) which had obvious cladding cracks, were leak tested with a helium mass spectrometer. Each fuel pin was placed in a vacuum-tight pressure vessel. The vessel was evacuated and then pressurized with helium to 2.8×10^5 newtons per square meter (40 psi) gage pressure for several minutes. The pin was transferred to another vessel which then was evacuated. When the pressure was reduced to about 6.6×10^3 newtons per square meter (50 torr), the gas in the vessel was checked with a helium mass spectrometer. Two clean, polished rods similar in size to the fuel pins were used as "no leak" standards to check the procedure. The leak testing results are presented in table V.

The weight measurements made before and after irradiation (table V) confirm that no NaK had penetrated the cladding of any of the fuel pins except pins 12 and 14 (T-111 and 95 percent dense UN) which were known to have cracked claddings. There were no cladding openings large enough to allow NaK to enter any of the other seven fuel pins.

Fuel Pin Puncture and Disassembly

Prior to puncturing the fuel pins for fission gas measurement and sampling, a gamma scan was run on each of the fuel pins selected for the extensive examination. The scan was used in conjunction with isotopic burnup analysis to obtain an axial burnup profile. This is described later in the Burnup Analysis section.

Each fuel pin, except pin 14 (T-111 and 95 percent dense UN), was sealed in a vacuum chamber. The fuel pin cladding was punctured into the void space above the top fuel pellet. This puncture was about 0.97 centimeter (0.37 in.) below the top of the upper end cap. The calculated fuel pin gas pressures and calculated percent fission gas released from the fuel for each of these three pins are presented in table VI. These data show high fission gas release from the UO_2 fuel and relatively low release from the UN.

For disassembly the fuel pin was clamped inside a split Cb-1Zr block which is drilled to hold and position the pin. The block and the fuel pin were then cut with a power hacksaw. The saw was operated for 10 seconds and then stopped for 50 seconds to avoid heating the block and the fuel pin excessively.

Fuel pin 11 (T-111 and 85 percent dense UN) was the first to be disassembled. Both end caps were sawed off, and an attempt was made to remove the fuel pellets by gently

tapping one end of the fuel pin while it was in a vertical position. The fuel pellets could not be removed in this manner. The fuel pin was then cut through the axial midpoint and four 0.6-centimeter- (0.25-in. -) wide rings of cladding and fuel were cut from the two pieces. Two samples were cut from each side of the midaxis cut. The sample closest to the top of the pin was labeled 1, and the sample closest to the bottom of the fuel pin was labeled 4. The four samples composed the center 3.17-centimeter (1.25-in.) section of the fuel pin. Samples were then cut from fuel pins 14, 17, and 18 in the same manner. Some of the severely cracked UO_2 fuel fell apart during the sawing operation. Each sample was stored in a vial which was placed in a dessicator under an argon atmosphere.

The four samples from each fuel pin were used as follows:

Sample 1: Fuel density and cladding ductility tests

Sample 2: Fuel burnup and cladding ductility tests

Sample 3: Spare fuel and cladding - not examined

Sample 4: Metallographic examination of both fuel and cladding

Burnup Analysis

Axial burnup profiles were determined for each of the four fuel pins. Prior to disassembly, a gamma scan was run along the axis of each fuel pin. The gamma scan facility incorporated a high resolution germanium-lithium drifted diode detector. A collimator with an adjustable slit (varied in width from 2.54 to 0.254 cm (1 to 0.1 in.)) penetrated the wall of the hot lab cell. The pin being scanned was positioned in a chuck to allow rotation and linear axial movement of the sample being scanned. For the four pins which were examined, the collimator slit width was 0.254 centimeter (0.1 in.), and the relative burnup along the axis of each pin was determined by measuring gamma radiation from Cb-95. The scan of Cb-95 gamma intensities was calibrated by means of a mass spectrometer analysis of a sample of fuel from each pin. The absolute value of the burnup at the location of the sample was calculated by determining the amount of neodymium-148 and the U-235 to U-236 ratio.

A typical axial burnup profile is presented in figure 7 (for fuel pin 11). The burnup values, calculated from the heat generation values measured with the calorimeters, and the average of measured burnup values for all four pins are given in table VII. Comparing the calculated and measured values shows close agreement for some pins (such as for fuel pin 11) but large differences for others (such as for fuel pin 17). The measured values are taken to be more accurate than the calculated values.

Cladding Ductility Tests

Ductility tests were made on two cladding samples from each fuel pin. Previous work (ref. 21) has shown that T-111, aged at temperatures near 1040° C for extended periods of time (~1000 hr or greater) becomes sensitized to hydrogen embrittlement. Small amounts of hydrogen (bulk analysis on the order of 2 ppm or less by weight) can cause a severe reduction in ductility. Straining the sensitized alloy in a humid atmosphere also was shown to result in brittle failure. To prevent ambiguous ductility test results, testing was carried out in a dry argon atmosphere. One sample from each fuel pin was tested in the as-irradiated condition, and one sample was tested after being heated in a vacuum furnace at 1040° C for 1 hour. It is known from out-of-reactor studies that this vacuum annealing will restore the ductility to hydrogen embrittled T-111 (ref. 21).

Pictures of the ring expansion test (ductility test) components are shown in figure 8. The procedure for testing the cladding ductility was to cut a ring about 0.635 centimeter (0.25 in.) in width from the cladding, smooth the cut surfaces with a file, and dry sand the filed surfaces with silicon carbide paper. The ring was placed over a stainless steel expansion mandrel which had a tapered hole through the center. A hardened tool steel tapered plug was fitted into the tapered hole, the assembly was placed in a plastic bag containing a dessicant. This plastic bag was then purged with argon for 30 minutes. Following the purging a tensile test machine forced the tapered plug into the stainless steel expansion mandrel at a rate of 0.051 centimeter per minute (0.02 in./min). This expanded the mandrel and the cladding ring at a diametral strain rate of 0.0051 centimeter per minute (0.002 in./min). Extensiometers were placed on the cladding ring surfaces before the test was started, and both diameter and force were recorded with a two pen recorder. The diameter at fracture was determined both from the extensiometer reading on the chart and from the measurement of the diameter of the stainless steel cylinder with precision micrometers.

The results of the ductility tests are listed in table VIII. All T-111 cladding specimens were found to be brittle in the as-irradiated condition. The two T-111 specimens from the UN-fueled pins were ductile after a 1-hour heat treatment at 1040° C in a vacuum furnace. But the T-111 cladding from the UO_2 fueled pin (pin 17) remained brittle. The Cb-1Zr cladding was ductile in both the as-irradiated and vacuum-annealed conditions.

Metallographic Examination of Cladding

A sample from each of the fuel pins was examined by optical metallography for structural changes, reactions, and cracks in the cladding or liner. The etchants used are the following:

Material	Etchant
Tungsten	Murikami's
T-111	30 g $NH_4 \cdot HF_2$ 50 ml HNO_3 (71 percent) 20 ml H_2O
Cb-1Zr	30 ml glycerine 30 ml HNO_3 (71 percent) 10 ml HF (49 percent)
UN	60 ml lactic acid (85 percent) 24 ml HNO_3 (71 percent) 2 ml HF (49 percent)
UO_2	10 ml H_2SO_4 (95 percent) 90 ml H_2O_2 (30 percent)

The cladding from the four fuel pins showed no major structural change as compared to the unirradiated cladding. The grain size of the T-111 and Cb-1Zr both before and after irradiation ranged from ASTM grain size 5 to 6 (0.05 to 0.77 mm diam). No reactions between either the fuel and cladding or the liner and the cladding are visible in the photomicrographs of the T-111/UN fuel pins (pin 14 or 11, see figs. 9(a) and (b)). But slight erosion of the cladding was observed in both of the UO_2 fueled pins: figures 10 and 11 show sections of cladding from fuel pins 17 (T-111 and 95 percent dense UO_2) and 18 (Cb-1Zr and 95 percent dense UO_2) where the liner was cracked. A very slight layer (less than 0.0003 cm thick) is visible on the inner surface of the Cb-1Zr cladding in figure 11. This may be vapor transported fuel or solid fission products.

The crack in the T-111 cladding of fuel pin 14 (T-111 and 95 percent dense UN) (shown in figs. 12 and 13(a)) appears to be an intergranular crack. A second crack, which initiated at the inside of the cladding but did not propagate all the way through the cladding, is shown in figure 13(b).

Microstructure of Fuel

Figure 14 shows etched microstructures of the three types of fuel (85 and 95 percent dense UN and 95 percent dense UO_2) in the unirradiated aged condition. Unetched photomicrographs of the UN fuel from irradiated fuel pins 11 (T-111 and 85 percent dense UN) and 14 (T-111 and 95 percent dense UN) are shown in figures 15 and 16. In figure 16 the large grains of the irradiated 95 percent dense UN are outlined with fission gas bubbles

(see ref. 7). The larger voids are as-fabricated porosity. Grain delineation by fission gas bubbles was not visible in the irradiated 85 percent dense UN (fig. 15). Figures 17 and 18 show the same UN specimens that are shown in figures 15 and 16 but in the etched condition. Some unidentified second-phase particles were visible in the 85 percent dense UN (fig. 17). These particles are very fine (~0.08-mm (0.0012-in.) diam) and are sparsely distributed. It is possible that this phase consists of oxide particles formed in the fabrication of the pellets - although none were observed in the thermally aged sample (see fig. 14(b)). No second phase was observed in the larger grained 95 percent dense UN fuel (see fig. 18).

There was no grain growth of the UN fuel in either of the two pins. And there were no lenticular voids or columnar grains which would result from the movement of voids up a temperature gradient.

The UO_2 fuel from pins 17 (T-111 and 95 percent dense UO_2) and 18 (Cb-1Zr and 95 percent dense UO_2) showed essentially the same features as the UN fuel (i.e., no grain growth, no lenticular voids, and no columnar grains). However, figure 19 shows a cross section of a UO_2 fuel cylinder from pin 18 (Cb-1Zr and 95 percent dense UO_2). It is apparent that the number of voids increased toward the axial centerline of the pellet. These voids may be from grain pullout suggesting weak grain boundaries (possibly from accumulation of fission gas), or they may result from the movement of voids up the temperature gradient. This gradient of void concentration was not observed in the irradiated low density UN (see fig. 20) or in the irradiated high density UN.

Fuel Density Measurements

Density measurements were made on irradiated UN fuel from pins 11 (T-111 and 85 percent dense UN) and 14 (T-111 and 95 percent dense UN) by immersion in carbon tetrachloride (CCl_4) employing a Westphal balance. For porous UN, measurements with a mercury pycnometer would have been preferable to CCl_4 immersion (which tends to give values which are too high), but the necessary mercury pycnometer apparatus was not available in the hot cells. The density of the UN also was calculated from the diameter and weight of preirradiated and postirradiated fuel assuming isotropic swelling behavior. These density values would tend to be too low if there are cracks in the fuel.

These two methods of density measurement, considering that the irradiated UN pellets were cracked and that the 95 percent dense UN probably also contained interconnected porosity in the grain boundaries, gave qualitative information. But since one method would tend to give high density results (CCl_4 immersion) and the other would tend to give lower density readings, the results should bracket the actual density values for the irradiated fuels.

The density determinations for the UN pellets are listed in table IX. The density of the high density fuel (from pin 14) decreased considerably. This is probably due to the collection of the fission gases in the closed porosity and the resultant swelling of the fuel. Conversely, the density of the lower density fuel (from pin 11) remained at about the same level. In this case the porosity in the as-fabricated fuel was largely interconnected and thereby offered an easy route for release of the fission gases generated or for local accommodation of the swelling fuel. Density measurements were not made on irradiated UO_2 because the UO_2 cylinders crumbled into small pieces when an attempt was made to remove them from the fuel pins.

Thermal Simulation Pins

The visual appearance of the eight thermal simulation pins was unchanged by testing. When leak checking with a helium mass spectrometer none of these pins were found to contain leaks. A description of the thermal simulation pins is presented in table II. Four of these pins were examined for possible effects of thermal aging or thermal cycling to establish a baseline against which irradiation effects could be compared. These four thermal simulation pins were identical to the four irradiated pins examined in detail. The possible changes looked for in these thermal control test pins were (1) fuel and cladding microstructural changes, (2) fuel liner cladding reactions, and (3) fuel sintering from long-time exposure at the design concept operating temperature.

The four thermal simulation pins examined were designated S-7, S-8, S-17, and S-18. The examination consisted of the following:

(1) Dimension of the cladding
(2) Weight of the fuel pins
(3) Fuel pellet weight
(4) Fuel pellet dimensions
(5) Fuel pellet density (calculated from weight and dimensions)
(6) Cladding ductility tests
(7) Oxygen, nitrogen, and hydrogen analyses of cladding
(8) Optical metallography

All eight fuel pins were weighed to ±0.0005 gram, and their diameters measured to ±0.0005 centimeter (±0.0002 in.). The pretest dimensional measurements for the UN fueled simulation pins and the measurements of the dimensions of the UO_2 fueled pins were made by two different observers. All of the readings, both pretest and posttest, were made with precision micrometers calibrated against standards. The measurements are presented in appendix C.

The top end cap of each fuel pin was removed by cutting through the cladding wall about 0.317 centimeter (0.125 in.) below the end cap closure weld. The end cap was then

removed from the pin, and the internal parts of the pin were removed, packaged in glass containers, and labeled.

Each fuel pellet was weighed, and its dimensions were measured across the diameter and length. The fuel pellet dimensional measurements agreed to within 0.0013 centimeter (0.0005 in.) on the average. The weight measurements of the pretest and posttest conditions agreed to within 0.002 gram. Density measurements for each fuel pellet, calculated from the posttest dimensional and weight measurements, were in agreement with the pretest densities to within 0.2 percent.

Four 0.64-centimeter- (0.25-in.-) wide rings of cladding were cut with a hacksaw from each fuel pin, and the cut surfaces were filed to remove all burrs and cutting marks. The filed surfaces then were dry sanded with silicon carbide paper through 600-grit paper. One of these rings from each fuel pin was crushed in a vise in humid air (~50 percent relative humidity). All of the T-111 rings cracked before they could be fully flattened. The Cb-1Zr ring flattened completely without cracking. Another prepared ring from each fuel pin was crushed in a vise in a dry argon atmosphere. All of these rings flattened completely without cracking. Two extra rings from each fuel pin were retained in case further ductility tests were required.

One sample of cladding material from each fuel pin was analyzed for oxygen, hydrogen, and nitrogen. The samples, in preparation for analysis, were degreased and the tungsten liner was removed. The oxygen and nitrogen were determined using an inert gas fusion analyzer. The hydrogen was determined by vacuum fusion analysis. The pretest and posttest interstitial concentrations are listed in table X. It appears from the data that more oxygen contamination was picked up by the cladding from the UO_2 fuel than from the UN fuel in these tests. About the same amount of nitrogen was picked up by the cladding in the case of both fuels. The apparently higher contamination level of oxygen in the Cb-1Zr (on a weight percent basis) is due in part to the lower density of this metal as compared to the T-111.

Metallographic examination revealed no unusual change in microstructure. The aged cladding (fig. 21) and fuel (fig. 14) both appear as expected from previous observations for aged cladding and aged fuel.

DISCUSSION OF RESULTS

Fuel Pin Diametral Strain

Table XI summarizes the cladding diametral strains and the calculated burnups for all nine irradiated fuel pins. (The measured burnup also is given for pins 11, 14, 17, and 18.) These results indicate that three of the four fuel/cladding combinations tested

swelled less than the 1 percent strain limit and show promise for use in long-life reactors.

The T-111 cladding of the four fuel pins containing 85 percent dense UN (pins 10, 11, 13, and 15) was diametrally strained less than 0.5 percent at burnups nearly equivalent to that of the reactor design concept end-of-life value (~3 at. %). The fuel pins containing 95 percent dense UO_2 (pins 16, 17, and 18), at burnups of approximately 2 atom percent, exhibited somewhat greater diametral swelling than the 85 percent dense UN fuel pins. But the diametral swelling of the UO_2 pins also met the general goal of a 1 percent maximum strain limit with either T-111 or Cb-1Zr cladding.

The diametral increases in pins containing 95 percent dense UN fuel (pins 12 and 14) were larger than expected. Calculations of fuel pin swelling, using the CYGRO-2 analytical model (ref. 22), and the best available physical and mechanical property data predicted a maximum diametral strain of approximately 0.3 percent for a T-111 clad 95 percent dense fuel pin after 50 000 hours of irradiation to a burnup of 2.6 percent. However, both of these fuel pins swelled diametrally at least 1.5 percent before cracking. This large discrepancy between the calculated strain value and the experimental strain value could be due to the use of physical properties data (e.g., fuel thermal conductivity or fuel surface tension) or mechanical properties data (e.g., fuel creep, cladding creep) which may not be correct or may be affected by the irradiation environment to such an extent that the data measured may not be valid for the conditions of this test.

The postirradiation diametral increases measured for the cracked fuel pins include a sizable diameter increase after the cracking occurred - probably from unrestrained fuel swelling. Thus, it is important to know the diametral strain on the cladding when the crack initiated. This was estimated in two different ways. The axial profile of the outside of the cladding of fuel pin number 14, diametrically opposite the crack, was traced with a dial gage and the profile was plotted. The largest increase in radius was assumed to be representative of the average strain of the cladding at that axial point when the crack occurred. The measured value of cladding strain from this profile was 1.5 percent. Also, the crack width was measured (fig. 12), and the increase in diameter of the fuel pin cladding due to the opening of the crack alone was calculated. This value was then subtracted from the measured diametral increase to give the cladding diameter with the crack completely closed. The strain value when the crack initiated, as determined by this method, was 1.9 percent for fuel pin 14.

These estimates of cladding strain at the time the cladding cracked show that the cladding material (T-111) for the cracked pins exceeded the design concept goal of a maximum of 1 percent strain after 50 000 hours of irradiation. The cladding was probably strained at least 1.5 percent before cracking which was assumed to have occurred at approximately 8500 hours of irradiation. (As pointed out earlier, fission gas was detected in capsule UN-5 at about 8500 hours after irradiation was started). The cracking of the T-111 cladding on the 95 percent dense UN fuel pins is believed to have occurred because

of excessive fuel swelling coupled with embrittlement of the T-111. Although embrittled, the T-111 cladding of pins containing 85 percent dense UN was not strained enough to cause cracking, probably because of the lower density and lower compressive creep strength of the fuel which allowed release of the fission gases and/or internal creep of the fuels.

Cladding Embrittlement

Previous studies (e.g., ref. 21) indicate that very small bulk concentrations of hydrogen (~2 ppm by weight) are sufficient to reduce the room temperature ductility of T-111 from values of over 25 percent tensile elongation to very low values if the T-111 has been aged for times in excess of 1000 hours at about 1040° C. This was confirmed in this present series of tests by the thermal simulation fuel pin cladding ductility tests. These indicated T-111 sensitivity to hydrogen embrittlement as evidenced by the brittle fracture of test specimens in humid air and complete ductile behavior when strained in dry argon.

All irradiated T-111 cladding was brittle with diametral strains of 1 percent or less when strained in the as-irradiated condition in dry argon. All T-111 cladding samples from fuel pins which contained UN regained their ductility after a 1-hour vacuum anneal at 1040° C. The vacuum annealing was done to remove the hydrogen from the cladding samples. The hydrogen in the cladding is thought to have originated from the known reaction of neutrons with the nitrogen in the UN fuel, $\left\{N^{14}(n,p)C^{14}\right\}$. A sample calculation of the amount of hydrogen expected from this source is outlined in appendix D. The amount formed, equivalent to 5.0 ppm by weight, is sufficient to embrittle the T-111. The cold stainless steel containment vessel of the irradiation capsule prevented the escape of hydrogen generated within the capsule. This hydrogen was then absorbed by the T-111 on cooling. Direct irradiation damage of the cladding at these fluences by thermal neutrons would be expected to be slight, and it is not expected that such damage would be annealed out at the relatively low temperature (1040° C) used in the hydrogen removal vacuum heat treatment.

The T-111 cladding from the fuel pin containing the UO_2 fuel was brittle in both the as-irradiated and vacuum annealed conditions. But the cladding from the companion thermal simulation pin was ductile. Therefore, the cause for the embrittlement of the irradiated cladding was probably something other than hydrogen. The T-111 may have been contaminated by the UO_2 fuel (which could have been brought to the cladding by vapor phase transport) to form oxides of tantalum and hafnium and perhaps free uranium in the cladding during the irradiation. Embrittlement of T-111 by oxygen doping at temperatures between 850° and 1000° C has been shown to occur (ref. 23). The embrittlement may also have been due to fission products contaminating the cladding -

this is considered less likely than oxygen transport. The Cb-1Zr from the UO_2 fuel pin was ductile in both the as-irradiated and vacuum annealed condition.

In general, the results of the ring expansion tests (cladding ductility tests) of both irradiated and thermally aged fuel pin cladding show the following under the conditions of these tests:

(1) There was no observable reaction between the T-111 cladding and the nitrogen in thermal equilibrium with the UN fuel or released during the fissioning of the UN fuel. (It has been found (ref. 24) that 500 ppm by weight of nitrogen is necessary to embrittle T-111 at room temperature. It is assumed that nitrogen pickup was less than this value.)

(2) There was a reaction between the T-111 cladding and either fission products or UO_2 fuel which may have been transported to contact the cladding (vaporization and condensation, or extrusion through tungsten liner cracks). This reaction has caused the cladding to be brittle at room temperature.

(3) There was no noticeable reaction between the Cb-1Zr cladding and either the UO_2 fuel fission products or fuel which may have been transported to contact the cladding.

The embrittlement results which are attributed to hydrogen are a consequence of the test design and not the reactor design concept. The design of the test capsule is such that the hydrogen is retained within the capsule as it is generated and then it can be gettered by the T-111 as it cools. In the actual space power reactor concept, the hydrogen could not accumulate because it would permeate through the hot T-111 cladding into the lithium coolant loop and then through the hot T-111 pressure vessel and pipe walls and be lost in the vacuum of space. The test conditions then, as related to the hydrogen environment of the fuel pins, are not fully representative of the actual operating conditions of the reactor concept. Thus, it is likely that the T-111 embrittlement encountered in these tests would not be a problem in the actual space power reactor systems.

UN Fuel Density Effects

All of the UN fueled pins were designed to have the same smear density of fuel within the pin regardless of the density of fuel contained within the pin. The smear densities of the two different densities of fuel were equalized by including a central axial hole of appropriate size in the 95 percent dense UN pellets. Total fission gas generation should have been equivalent for the UN fuel pins of different fuel densities but equal burnups. However, the amount of fission gas released from porous and dense fuel would be expected to be different. No fuel pin gas volume measurements were made of the gases in the 95 percent dense UN fuel pins after testing because the cladding of both pins was cracked and the fission gases released from the fuel were lost during the irradiation. However, information from another fuel irradiation program (ref. 6) indicates about 2 percent projected fission gas release at comparable burnups for 95 percent dense UN

fuel under the conditions of this test. Also, calculations made during the latter part of the irradiation tests (based on the NaK cover gas activity and the capsule internal volume) indicated a fission gas release of less than 0.01 percent. (These calculations were approximate in nature and may have been in error.) A gas volume measurement was made of the gas in the 85 percent dense UN fuel pin (pin 11), and the fission gas release was calculated to be 4.3 percent. This difference in fission gas release is consistent with the hypothesis previously made to explain the greater swelling of the high density fuel.

Cracking occurred in the fuel pellets of both densities of UN fuel. There were circumferential cracks in both types of UN fuel. These may have propagated from very small circumferential cracks which were typical of those in as-fabricated fuel pellets prepared by the uniaxial dry pressing technique. Improvements in fabrication techniques developed after these pellets were fabricated could eliminate these small flaws in future pellet fabrication (ref. 17). In addition to these small transverse (circumferential) cracks, the 95 percent dense UN fuel contained longitudinal cracks which probably resulted from fuel swelling due to entrapped fission gases.

The most important comparison between the two types of fuels is that both fuel pins containing 95 percent dense UN fuel developed major cladding cracks during irradiation while none of the 85 percent dense UN fuel pins developed cladding cracks. Also, the 95 percent dense fuel pins apparently underwent diametral cladding strains prior to cracking as much as three times greater than the cladding strains produced in the 85 percent dense UN fuel pins at the end of irradiation. From figures 16 and 17 it may be inferred that the fission gases retained in the fuel during irradiation may have been accommodated more easily by the 85 percent dense UN fuel than by the 95 percent dense UN fuel. The grain boundaries in the 95 percent dense UN fuel clearly contained fission gas bubbles (fig. 16). In the 85 percent dense UN no fission gas bubbles were observed in the grain boundaries (fig. 17). Apparently the fission gases in the lower density fuel are either within the grains or have migrated into the open porosity, perhaps by way of the grain boundaries. Thus, it is likely that the distributed porosity in the lower density UN leads to greater release of fission gases and/or local accommodation of fuel swelling and the resulting transmission of less stress to the cladding.

It is concluded that the 85 percent dense UN offers more promise for successful design of a fuel pin for the reactor concept under consideration than does 95 percent dense UN.

Comparison of UN and UO_2

The UN itself did not contaminate the T-111 cladding nor degrade it under the conditions of this test. It appears that the UO_2 contaminated the T-111 cladding in fuel pin number 17 (T-111 and 95 percent dense UO_2), since the loss of ductility occurred during

the irradiation and the ductility could not be restored by outgassing in vacuum at 1040° C. It appears that some reaction of the UO_2 occurred with the cladding where there were tungsten liner cracks (see fig. 10). Also, contamination of the cladding with oxygen, apparently from the fuel, was noted in the companion thermal simulation test pins.

Both the UN fuel and the UO_2 fuel cracked during irradiation; however, the UO_2 fuel showed more severe cracking and the cracking occurred earlier in the irradiation test for the UO_2 than for the UN pins. Not only did the UO_2 crack more severely during irradiation, but it crumbled when fuel removal was attempted during fuel pin disassembly. Figure 19 shows a transverse section of an intact portion of UO_2 from fuel pin number 18 (Cb-1Zr and 95 percent dense UO_2). This photomicrograph shows a gradient of voids along the radius of the fuel pellet. These voids may be due to either grain pullout or fission gas voids. If the voids result from pullout, they denote weak grain boundaries and suggest the reason for fuel crumbling.

No comparison of fuel pellet swelling (including swelling into the central hole) could be made between the UN and UO_2 because the UO_2 fuel broke apart when attempts were made to remove samples from the cladding rings.

The fission gas release from the 95 percent dense UO_2 was six to eight times as great as the fission gas release from the 85 percent dense UN. At an assumed average fuel pin gas temperature of 990° C the internal gas pressure in fuel pin 18 (Cb-1Zr and 95 percent dense UO_2) was calculated to be 1.66×10^6 newtons per square meter (243 psi) at the end of the irradiation test. This final pressure was balanced in part by the NaK cover gas pressure of 1.551×10^6 newtons per square meter (225 psi). The difference of 1.27×10^5 newtons per square meter (18 psi) between the internal and external pressure should not have caused an increase in diameter of the Cb-1Zr cladding. In the case of an actual fuel pin, however, lithium is the coolant and requires an overpressure of only 1.38×10^5 newtons per square meter (20 psi) to prevent boiling. In this case, the fission gas pressure over UO_2 would become significant in stressing the cladding. Calculations indicate that this increase in fission gas pressure (0 to 1.66×10^6 N/m^2) over 50 000 hours would result in a Cb-1Zr cladding diametral strain greater than 5 percent (see appendix E for the calculations).

In order to reduce this substantial cladding diametral strain which would be deleterious to successful operation of the fuel pin, some method would be required to compensate for the internal fission gas pressure buildup (e.g., fuel pin venting, or cladding alloy strengthening).

Of the three types of fuel, the 85 percent dense UN appears to be more promising than either the 95 percent dense UO_2 or the 95 percent dense UN under the conditions of the tests performed in this study. The UO_2 has problems of severe cracking, excessive fission gas release, and possible cladding reactions associated with its use. Also, the UO_2 is reactive with the lithium reactor coolant. To determine the possibility of using

UO_2 as the fuel in the advanced space power reactor concept would require further testing, T-111 might have to be excluded as a cladding material, and a coolant other than lithium would have to be used.

Comparison of Cladding Materials

The irradiation tests provided a means for comparing T-111 with Cb-1Zr as the cladding material for 95 percent dense UO_2 fuel pins. Figures 9 and 10 show photomicrographs of the T-111 and Cb-1Zr cladding at areas where the tungsten liner had cracked during the irradiation test. Slight erosion of both materials is evident. Room temperature ductility tests showed no loss of ductility for the Cb-1Zr, but the T-111 was brittle.

During irradiation the T-111 cladding on the UO_2 apparently was contaminated and its mechanical properties were changed. It is believed that the contamination was from vapor transported fuel which reacted with the T-111 cladding to form the oxides of tantalum and hafnium and possibly free uranium. Under the conditions of this test, T-111 appears to be unacceptable as a cladding material for UO_2 fuel. In the case of an actual space power reactor, it is possible that the great affinity of lithium (used as a coolant in the reactor design concept) for oxygen would result in the transfer of oxygen from the cladding to the lithium during operation and maintain a low level of oxygen in the T-111 (ref. 25). However, free uranium might accumulate and damage the cladding.

No degradation of the mechanical properties of the Cb-1Zr cladding occurred as a result of the irradiation test, and the cladding diametral increase was within the acceptable level. Therefore, Cb-1Zr appears to be a promising candidate as a cladding material for 95 percent dense UO_2 fuel pins under these conditions. However, the presence of the eroded area at the tungsten liner crack in figure 11 indicates the need for more testing to prove its acceptability as a cladding material. Since the Cb-1Zr cladding was exposed to the UO_2 for only 8333 hours during this test, there also is the possibility that the erosion observed at the cladding cracks could become large enough to affect the cladding integrity after times up to 50 000 hours. Compatibility tests with Cb-1Zr and UO_2 might, therefore, be needed with liners containing defects for times up to 50 000 hours (or under conditions which better simulate the effect of this long term exposure). The Cb-1Zr alloy has a relatively low strength at 990° C; so any overtemperature operating conditions could result in diametral swelling of greater magnitude than was found under these test conditions. Also, the low strength of the alloy gives it low "growth potential" in relation to cladding temperature increases.

Comparison With Other Irradiation Tests

Other fuels irradiation work at the Lewis Research Center's Plum Brook Facility was carried out under conditions comparable to those of this investigation except that attention was confined primarily to 95 percent dense UN fuel clad with T-111 (refs. 5 and 6). Those results are in general agreement with those reported here on dense UN clad with T-111 in the following respects:

(1) The cladding was embrittled during the irradiation testing. The cause of the embrittlement was attributed to sensitization of the T-111 to hydrogen embrittlement at the irradiation temperature and absorption by the T-111 of hydrogen formed from an n, p reaction with the nitrogen in the UN fuel.

(2) Cladding cracks developed after small cladding strains and burnups from 2.1 to 2.6 percent heavy metal atoms.

(3) Fission gas release was probably less than 0.5 percent (refs. 5, 6, and 8).

(4) Significant fuel swelling occurred.

(5) No fuel-cladding or fission product-cladding reactions were observed with optical metallography.

In a study conducted by ORNL (ref. 11), irradiation at about 1400° C of pins consisting of 95 percent dense UN clad with T-111 led to cracking of the T-111 cladding at diametral strains of less than 1 percent. The reason for cracking of the cladding at this high temperature has not been established and may be different than for the cracking occurring at 990° C discussed in this report.

Battelle Memorial Laboratories (ref. 12) and Lawrence Radiation Laboratories (ref. 13) also irradiated UN fuel pins with refractory metal claddings (primarily tungsten or tungsten alloys). Their interest was primarily in higher temperatures (~1200° to 1800° C). One important conclusion of their work was that stable interconnected porosity in the fuel will reduce fuel pin swelling: this is in agreement with the results presented here for lower temperature tests.

Extensive irradiation testing of columbium alloy clad, high density UN at cladding temperatures from about 800° to 1200° C (mostly between 1100° and 1200° C) was carried out previously by Pratt and Whitney Aircraft - Connecticut Advanced Nuclear Engineering Laboratory (PWAC - CANEL) (ref. 9) and ORNL (ref. 10). Generally the diametral strain for Cb-1Zr clad pins was in excess of 1 percent at fuel burnups of ~2.5 percent or more. But for pins with a carbon-strengthened alloy cladding (i.e., Cb-1Zr-0.1C) tested in the 800° to 1000° C temperature range for times to about 10 000 hours and burnups of about 2 to 3 atom percent, the diametral strain was around 1 percent or less. Cracking of the cladding did not appear to be a problem for the columbium alloys. Therefore, columbium alloys could be considered for use in reactor designs that permit greater than 1 percent fuel pin diametral strain and/or where increases in operating temperatures are

not contemplated. The performance of columbium alloy clad UN pins also probably could be improved by using low density UN fuel with stable interconnected porosity.

However, the use of low density UN with stable interconnected porosity and clad with T-111 appears to offer the best promise of meeting the advanced space power reactor goals aimed at in the present study.

Comparison of Irradiation Test and Reactor Concept Conditions

One of the purposes of this investigation was to select the most promising fuel-cladding combinations for further development and to identify potential problems. Potential problems not identified in this test program may appear under actual reactor design operating conditions. In the design of this experiment there are a number of areas where actual reactor conditions were not reproduced:

(1) Accelerated burnup rates were used (acceleration factors of about 5 for UN pins and 6.25 for the UO_2 pins). These higher rates may not have allowed enough time for chemical compatibility problems to develop as they might during 50 000 hours of operation.

(2) The fast neutron fluence was at least an order of magnitude less than that which a space power reactor would experience. The higher fluence level may have an important effect on the possible radiation damage (a concommittant effect on mechanical properties) experienced by the fuel pin cladding material.

(3) The fuel pins were exposed to NaK rather than lithium. Lithium has been shown to deplete T-111 of oxygen and thereby to decrease the creep strength of T-111.

(4) The fuel pins in their NaK containers were irradiated in an inert gas atmosphere containing hydrogen which slowly increased in concentration over the duration of the irradiation. In an actual reactor the hydrogen produced in the fuel during operation would be lost to the coolant and/or the vacuum of space. Thus, no appreciable hydrogen concentrations would accumulate in the fuel pins.

To more closely reproduce the actual reactor concept conditions, future fuel pin irradiation testing should be done in a fast-flux test facility. Also, the irradiation capsule design should incorporate a means for removing hydrogen during irradiation (e.g., gettering with zirconium, sweeping with inert gas, or a permeation membrane). Ideally, tests (e.g., compatibility, irradiation, mechanical properties) should be run for the design life of 50 000 hours in lithium. This suggests that work should begin long before a space power reactor is actually needed.

CONCLUSIONS

Nine refractory-metal-clad fuel pins containing either UN or UO_2 fuel were irradiated at a cladding temperature of about 990° C for times from 8333 to 10 450 hours and burnups from 1.76 to 3.11 heavy metal atom percent in the Oak Ridge reactor. Also, eight fuel pins were heated out-of-reactor as thermal controls. After preliminary observations of these pins, four of the irradiated and four of the corresponding thermal control fuel pins were evaluated as described in this report. The four irradiated pins and thermal control pins consisted of (1) 95 percent dense cylindrical UN compacts (with an axial hole) clad with tungsten-lined T-111, (2) 85 percent dense UN compacts clad with tungsten-lined T-111, (3) 95 percent dense UO_2 compacts (with an axial hole) clad with tungsten-lined T-111, and (4) 95 percent dense UO_2 compacts (with an axial hole) clad with tungsten-lined Cb-1Zr. Evaluating the irradiated fuel pins and comparing them to the thermal control pins led to the following major conclusions:

1. Low density (85 percent dense) UN fuel clad with tungsten-lined T-111 shows the greatest promise of meeting the 50 000-hour life goal for the fuel pin design concept with 1 percent or less diametral cladding strain. High density (95 percent dense) UN resulted in strains of about 1.5 percent or more and cladding cracks under the same test conditions.

2. The UO_2 fuel exhibited acceptably low levels of swelling in these tests. However, UO_2 does not appear attractive for this fuel pin design concept because of excessive cracking of the fuel, high fission gas release (~30 percent compared to ~4 percent for porous UN fuel), and reactions with T-111 and possibly with Cb-1Zr.

3. Embrittlement and cracking of the T-111 cladding of the UN fuel pins occurred under the irradiation test conditions used in this study. This embrittlement is thought to be caused primarily by sensitization of the T-111 to hydrogen embrittlement because of thermal aging and generation of hydrogen by the (n,p) reaction with nitrogen in the UN fuel. A strain of about 1.5 percent caused cracking of the hydrogen embrittled T-111 cladding. (The problem of hydrogen embrittlement is not expected to occur in an actual reactor because hydrogen will be lost by permeation through the hot reactor containment vessel.)

4. The Cb-1Zr exhibited less chemical compatibility problems than T-111 as a fuel cladding material. Therefore, Cb-1Zr should be investigated as an alternate cladding material for porous UN for fuel pins limited to cladding temperatures below about 990° C.

Lewis Research Center,
National Aeronautics and Space Administration,
Cleveland, Ohio, January 29, 1975,
501-21.

APPENDIX A

TEST FUEL PIN ASSEMBLY PROCEDURE

Both the irradiation test fuel pins and the thermal simulation pins were assembled using the following procedures:

(1) Thorough cleaning (degreasing and chemical cleaning) of all metal components
(2) Gas tungsten arc welding of bottom end cap to cladding tube (sample weld also made for chemical analysis and metallography)
(3) Inspection of welds including visual inspection, helium mass spectrometry leak testing, X-ray radiography, and dye penetrant testing
(4) Insertion of liners and loading of fuel pins with fuel and spacers
(5) Inspection of exterior of fuel pins for fuel contamination (cleaned by alcohol swab if contamination was present)
(6) Gas tungsten arc welding of top end cap in helium at 1 atmosphere pressure
(7) Inspection of final closure welds including visual inspection, helium leak testing, and X-ray radiography
(8) X-ray radiography to show positioning of fuel and spacers
(9) Measurement of fuel pin diameters, lengths, and weights
(10) Final degreasing and vacuum heat treatment at 1330° C for 1 hour

The degreasing operation consisted of washing with high purity acetone followed by an alcohol rinse. The chemical cleaning solutions were composed of nitric acid, sulfuric acid, hydrofluoric acid, and water (ref. 18).

APPENDIX B

PREIRRADIATION DIAMETER AND LENGTH MEASUREMENTS ON TEST FUEL PINS

FUEL PIN 10 (T-111 AND 85 PERCENT DENSE UN)

Distance from top weld, cm	Diameter, cm	
	Measurement location, deg	
	0	90
0 (next to weld at top)	0.9454	0.9464
1.27	.9459	.9459
2.54	.9456	.9459
3.81	.9454	.9454
5.08	.9451	.9459
6.35	.9449	.9454
7.62	.9449	.9454
8.89	.9454	.9454
10.16	.9451	.9459
11.43 (next to weld at bottom)	.9449	.9472

Reading number	Fuel pin length, cm	
	Weld to weld	Stem to stem
1	11.410	12.537
2	11.405	12.540
3	11.410	12.540
Average	11.407	12.540

FUEL PIN 11 (T-111 AND 85 PERCENT DENSE UN)

Distance from top weld, cm	Diameter, cm	
	Measurement location, deg	
	0	90
0 (next to weld at top)	0.9446	0.9444
1.27	.9446	.9446
2.54	.9449	.9449
3.81	.9446	.9449
5.08	.9446	.9444
6.35	.9444	.9439
7.62	.9441	.9439
8.89	.9444	.9436
10.16	.9439	.9439
11.43 (next to weld at bottom)	.9436	.9449

Reading number	Fuel pin length, cm	
	Weld to weld	Stem to stem
1	11.382	12.507
2	11.387	↓
3	11.397	
Average	11.389	

FUEL PIN 12 (T-111 AND 95 PERCENT DENSE UN)

Distance from top weld, cm	Diameter, cm	
	Measurement location, deg	
	0	90
0 (next to weld at top)	0.9464	0.9459
1.27	.9464	.9459
2.54	.9459	.9462
3.81	.9462	.9464
5.08	.9462	.9462
6.35	.9462	.9459
7.62	.9459	.9459
8.89	.9459	.9459
10.16	.9462	.9462
11.43 (next to weld at bottom)	.9467	.9462

Reading number	Fuel pin length, cm	
	Weld to weld	Stem to stem
1	11.377	12.835
2	11.384	↓
3	11.428	
Average	11.397	

FUEL PIN 13 (T-111 AND 85 PERCENT DENSE UN)

Distance from top weld, cm	Diameter, cm	
	Measurement location, deg	
	0	90
0 (next to weld at top)	0.9479	0.9472
1.27	.9474	.9472
2.54	.9474	.9477
3.81	.9472	.9479
5.08	.9479	.9482
6.35	.9477	↓
7.62	.9474	
8.89	.9477	
10.16	.9477	
11.43 (next to weld at bottom)	.9477	

Reading number	Fuel pin length, cm	
	Weld to weld	Stem to stem
1	11.384	12.537
2	11.394	12.537
3	11.407	12.543
Average	11.394	12.540

FUEL PIN 14 (T-111 AND 95 PERCENT DENSE UN)

Distance from top weld, cm	Diameter, cm	
	Measurement location, deg	
	0	90
0 (next to weld at top)	0.9464	0.9464
1.27	.9467	↓
2.54	.9467	↓
3.81	.9464	↓
5.08	.9464	.9462
6.35	.9464	.9464
7.62	.9462	.9459
8.89	.9456	.9456
10.16	.9479	.9467
11.43 (next to weld at bottom)	.9477	.9464

Reading number	Fuel pin length, cm	
	Weld to weld	Stem to stem
1	11.425	12.532
2	11.428	12.532
3	11.433	12.530
Average	11.428	12.530

FUEL PIN 15 (T-111 AND 85 PERCENT DENSE UN)

Distance from top weld, cm	Diameter, cm	
	Measurement location, deg	
	0	90
0 (next to weld at top)	0.9467	0.9477
1.27	.9467	.9469
2.54	.9472	.9467
3.81	.9464	.9464
5.08	↓	.9464
6.35	↓	.9456
7.62	↓	.9456
8.89	.9459	.9454
10.16	.9467	.9462
11.43 (next to weld at bottom)	.9477	.9469

Reading number	Fuel pin length, cm	
	Weld to weld	Stem to stem
1	11.394	12.865
2	11.397	↓
3	11.412	↓
Average	11.402	↓

FUEL PIN 16 (Cb-1Zr AND 95 PERCENT DENSE UO_2)

Distance from top weld, cm	Diameter, cm	
	Measurement location, deg	
	0	90
0 (next to weld at top)	0.9507	0.9510
1.27	.9510	.9512
2.54	.9505	.9510
3.81	.9512	.9507
5.08	.9507	.9507
6.35	.9507	.9505
7.62	.9497	.9502
8.89	.9502	.9505
10.16	.9507	.9510
11.43 (next to weld at bottom)	.9510	.9510

Reading number	Fuel pin length, cm	
	Weld to weld	Stem to stem
1	11.432	12.596
2	11.420	↓
3	11.445	↓
Average	11.432	↓

FUEL PIN 17 (T-111 AND 95 PERCENT DENSE UO_2)

Distance from top weld, cm	Diameter, cm	
	Measurement location, deg	
	0	90
0 (next to weld at top)	0.9469	0.9469
1.27	↓	↓
2.54	↓	↓
3.81	↓	↓
5.08	↓	↓
6.35	.9467	.9467
7.62	.9464	.9469
8.89	.9469	↓
10.16	.9464	↓
11.43 (next to weld at bottom)	.9467	↓

Reading number	Fuel pin length, cm	
	Weld to weld	Stem to stem
1	11.389	12.548
2	11.405	↓
3	11.410	↓
Average	11.402	↓

FUEL PIN 18 (Cb-1Zr AND 95 PERCENT DENSE UO_2)

Distance from top weld, cm	Diameter, cm	
	Measurement location, deg	
	0	90
0 (next to weld at top)	0.9525	0.9515
1.27	.9517	.9520
2.54	.9520	↓
3.81	.9525	↓
5.08	.9522	↓
6.35	.9510	↓
7.62	.9520	.9515
8.89	.9512	.9510
10.16	.9510	.9515
11.43 (next to weld at bottom)	.9510	.9510

Reading number	Fuel pin length, cm	
	Weld to weld	Stem to stem
1	11.400	12.847
2	11.410	↓
3	11.402	↓
Average	11.405	↓

APPENDIX C

OUT-OF-REACTOR THERMAL CONTROL FUEL PIN WEIGHTS AND DIMENSIONS

PRETEST

FUEL PIN S-18[a] (Cb-1Zr AND 95 PERCENT DENSE UO_2)

Distance from top weld, cm	Diameter, cm	
	Measurement location, deg	
	0	90
0 (next to weld at top)	0.9520	0.9512
1.27	.9517	.9517
2.54	.9520	.9520
3.81	.9520	.9520
5.08	.9520	.9517
6.35	.9515	↓
7.62	.9520	
8.89	.9520	
10.16	.9515	.9520
11.43 (next to weld at bottom)	.9522	.9510

Reading number	Fuel pin length, cm	
	Weld to weld	*Stem to stem*
1	11.402	12.568
2	11.412	↓
3	11.420	
Average	11.412	

[a]Weight, 69.883 g.

FUEL PIN S-17[a] (T-111 AND 95 PERCENT DENSE UO_2)

Distance from top weld, cm	Diameter, cm	
	Measurement location, deg	
	0	90
0 (next to weld at top)	0.9467	0.9474
1.27	.9472	.9469
2.54	.9474	.9469
3.81	.9469	.9469
5.08	.9469	.9464
6.35	.9479	.9469
7.62	.9472	.9469
8.89	.9469	.9469
10.16	.9462	.9456
11.43 (next to weld at bottom)	.9462	.9469

Reading number	Fuel pin length, cm	
	Weld to weld	Stem to stem
1	11.428	12.560
2	11.412	↓
3	11.410	
Average	11.415	

[a]Weight, 93.381 g.

POSTTEST

FUEL PIN S-18[a] (Cb-1Zr AND 95 PERCENT DENSE UO_2)

Distance from top weld, cm	Diameter, cm	
	Measurement location, deg	
	0	90
0 (next to weld at top)	0.9528	0.9525
1.27	.9517	.9520
2.54	.9520	.9525
3.81	.9517	.9517
5.08	.9517	.9515
6.35	.9522	.9522
7.62	.9520	.9517
8.89	.9517	.9517
10.16	.9515	.9515
11.43 (next to weld at bottom)	.9512	.9505

Reading number	Fuel pin length, cm	
	Weld to weld	Stem to stem
1	11.438	------
2	11.430	------
3	11.4226	------
Average	-------	------

[a]Weight, 69.884 g.

FUEL PIN S-17[a] (T-111 AND 95 PERCENT DENSE UO_2)

Distance from top weld, cm	Diameter, cm	
	Measurement location, deg	
	0	90
0 (next to weld at top)	0.9472	0.9467
1.27	.9472	.9474
2.54	.9472	.9472
3.81	.9474	.9477
5.08	.9472	.9469
6.35	.9472	.9469
7.62	.9472	.9472
8.89	.9456	.9462
10.16	.9462	.9459
11.43 (next to weld at bottom)	.9469	.9467

Reading number	Fuel pin length, cm	
	Weld to weld	Stem to stem
1	11.432	------
2	11.437	------
3	11.381	------
Average	11.417	------

[a]Weight, 93.377 g.

PRETEST

FUEL PIN S-16[a] (Cb-1Zr AND 95 PERCENT DENSE UO_2)

Distance from top weld, cm	Diameter, cm	
	Measurement location, deg	
	0	90
0 (next to weld at top)	0.9515	0.9517
1.27	↓	.9520
2.54	↓	.9515
3.81	↓	.9515
5.08	.9512	.9510
6.35	.9510	.9507
7.62	.9510	.9510
8.89	.9510	.9505
10.16	.9502	.9515
11.43 (next to weld at bottom)	.9502	.9502

Reading number	Fuel pin length, cm	
	Weld to weld	Stem to stem
1	11.432	12.535
2	11.410	↓
3	11.405	↓
Average	11.415	↓

[a]Weight, 69.583 g.

FUEL PIN S-9[a] (T-111 AND 95 PERCENT DENSE UN)

Distance from top weld, cm	Diameter, cm	
	Measurement location, deg	
	0	90
0 (next to weld at top)	0.9459	0.9462
1.27	.9462	.9462
2.54	.9462	.9456
3.81	.9454	.9454
5.08	.9454	.9454
6.35	.9464	.9459
7.62	.9456	.9446
8.89	.9454	.9449
10.16	.9451	.9449
11.43 (next to weld at bottom)	.9446	.9459

Reading number	Fuel pin length, cm	
	Weld to weld	Stem to stem
1	11.435	12.708
2	11.433	↓
3	11.435	↓
Average	11.435	↓

[a]Weight, 101.947 g.

POSTTEST

FUEL PIN S-16[a] (Cb-1Zr AND 95 PERCENT DENSE UO_2)

Distance from top weld, cm	Diameter, cm	
	Measurement location, deg	
	0	90
0 (next to weld at top)	0.9522	0.9510
1.27	.9510	.9520
2.54	.9510	.9517
3.81	.9512	.9512
5.08	.9505	.9507
6.35	.9507	.9510
7.62	.9507	.9505
8.89	.9512	.9512
10.16	.9507	.9507
11.43 (next to weld at bottom)	.9502	.9497

Reading number	Fuel pin length, cm	
	Weld to weld	Stem to stem
1	11.468	------
2	11.484	------
3	11.435	------
Average	11.462	------

[a]Weight, 69.584 g.

FUEL PIN S-9[a] (T-111 AND 95 PERCENT DENSE UN)

Distance from top weld, cm	Diameter, cm	
	Measurement location, deg	
	0	90
0 (next to weld at top)	0.9477	0.9479
1.27	.9477	.9474
2.54	.9472	.9469
3.81	.9467	.9469
5.08	.9472	.9479
6.35	.9469	.9464
7.62	.9459	.9472
8.89	.9464	.9469
10.16	.9459	.9467
11.43 (next to weld at bottom)	.9459	.9469

Reading number	Fuel pin length, cm	
	Weld to weld	Stem to stem
1	11.434	------
2	11.433	------
3	11.433	------
Average	11.433	------

[a]Weight, 101.947 g.

PRETEST

FUEL PIN S-8[a] T-111 AND 95 PERCENT DENSE UN)

Distance from top weld, cm	Diameter, cm	
	Measurement location, deg	
	0	90
0 (next to weld at top)	0.9439	0.9439
1.27	.9446	.9444
2.54	.9441	.9436
3.81	.9439	.9441
5.08	.9441	.9439
6.35	.9444	
7.62	.9446	
8.89	.9446	
10.16	.9446	
11.43 (next to weld at bottom)	.9456	.9451

Reading number	Fuel pin length, cm	
	Weld to weld	Stem to stem
1	11.453	12.705
2	11.453	12.703
3	11.458	12.703
Average	11.453	12.703

[a]Weight, 101.146 g.

FUEL PIN S-7[a] (T-111 AND 85 PERCENT DENSE UN)

Distance from top weld, cm	Diameter, cm	
	Measurement location, deg	
	0	90
0 (next to weld at top)	0.9454	0.9467
1.27	.9462	.9462
2.54	.9456	.9456
3.81	.9454	.9462
5.08	.9446	.9451
6.35	.9449	.9449
7.62	.9451	.9451
8.89	.9454	.9454
10.16	.9456	.9454
11.43 (next to weld at bottom)	.9479	.9469

Reading number	Fuel pin length, cm	
	Weld to weld	Stem to stem
1	11.453	12.705
2	11.443	12.708
3	11.450	12.705
Average	11.448	12.705

[a]Weight, 100.687 g.

POSTTEST

FUEL PIN S-8[a] (T-111 AND 95 PERCENT DENSE UN)

Distance from top weld, cm	Diameter, cm	
	Measurement location, deg	
	0	90
0 (next to weld at top)	0.9446	0.9454
1.27	.9449	.9454
2.54	.9449	.9451
3.81	.9451	.9456
5.08	.9444	.9456
6.35	.9451	.9456
7.62	.9451	.9459
8.89	.9454	.9462
10.16	.9459	.9454
11.43 (next to weld at bottom)	.9469	.9469

Reading number	Fuel pin length, cm	
	Weld to weld	Stem to stem
1	11.463	------
2	11.468	------
3	11.455	------
Average	11.462	------

[a]Weight, 101.146 g.

FUEL PIN S-7[a] (T-111 AND 85 PERCENT DENSE UN)

Distance from top weld, cm	Diameter, cm	
	Measurement location, deg	
	0	90
0	0.9489	0.9487
1.27	.9472	.9469
2.54	.9469	.9469
3.81	.9467	.9467
5.08	.9469	.9464
6.35	.9459	.9462
7.62	.9462	.9467
8.89	.9472	.9472
10.16	.9474	.9467
11.43 (next to weld at bottom)	.9477	.9477

Reading number	Fuel pin length, cm	
	Weld to weld	Stem to stem
1	11.468	------
2	11.450	------
3	11.460	------
Average	11.459	------

[a]Weight, 100.685 g.

PRETEST

FUEL PIN S-3[a] (T-111 AND 85 PERCENT DENSE UN)

Distance from top weld, cm	Diameter, cm	
	Measurement location, deg	
	0	90
0 (next to weld at top)	0.9454	0.9454
1.27	.9454	.9449
2.54	.9451	.9444
3.81	↓	.9444
5.08		.9451
6.35		.9449
7.62	.9454	.9451
8.89	.9451	.9454
10.16	.9451	.9451
11.43 (next to weld at bottom)	.9474	.9477

Reading number	Fuel pin length, cm	
	Weld to weld	Stem to stem
1	11.448	12.692
2	11.445	↓
3	11.440	
Average	11.445	

[a]Weight, 101.372 g.

FUEL PIN S-2[a] (T-111 AND 85 PERCENT DENSE UN)

Distance from top weld, cm	Diameter, cm	
	Measurement location, deg	
	0	90
0 (next to weld at top)	0.9459	0.9436
1.27	.9459	.9444
2.54	.9459	.9446
3.81	.9451	.9446
5.08	.9451	.9446
6.35	.9449	.9449
7.62	.9444	.9439
8.89	.9449	.9444
10.16	.9444	.9444
11.43 (next to weld at bottom)	.9469	.9472

Reading number	Fuel pin length, cm	
	Weld to weld	Stem to stem
1	11.460	12.700
2	11.453	↓
3	11.466	
Average	11.460	

[a]Weight, 101.246 g.

POSTTEST

FUEL PIN S-3[a] (T-111 AND 85 PERCENT DENSE UN)

Distance from top weld, cm	Diameter, cm	
	Measurement location, deg	
	0	90
0 (next to weld at top)	0.9469	0.9464
1.27	.9464	.9456
2.54	.9459	.9459
3.81	.9459	.9467
5.08	.9462	.9459
6.35	.9462	.9459
7.62	.9467	.9459
8.89	.9456	.9462
10.16	-----	-----
11.43 (next to weld at bottom)	.9474	.9451

Reading number	Fuel pin length, cm	
	Weld to weld	Stem to stem
1	11.455	------
2	11.458	------
3	11.463	------
Average	11.459	------

[a]Weight, 101.367 g.

FUEL PIN S-2[a] (T-111 AND 85 PERCENT DENSE UN)

Distance from top weld, cm	Diameter, cm	
	Measurement location, deg	
	0	90
0 (next to weld at top)	0.9451	0.9451
1.27	.9454	.9462
2.54	.9459	.9459
3.81	.9459	.9464
5.08	.9462	.9462
6.35	.9454	.9451
7.62	.9454	.9456
8.89	.9459	.9469
10.16	.9454	.9464
11.43 (next to weld at bottom)	.9459	.9479

Reading number	Fuel pin length, cm	
	Weld to weld	Stem to stem
1	11.468	------
2	11.463	------
3	11.471	------
Average	11.467	------

[a]Weight, 101.244 g.

APPENDIX D

SAMPLE CALCULATION OF AMOUNT OF HYDROGEN PRODUCTION FROM $\{N^{14}(n,p)C^{14}\}$ REACTION IN UN FUEL DURING IRRADIATION TESTS AT ORNL

Calculations were made to determine the amount of hydrogen produced in UN fuel during irradiation testing at ORNL. The source of the hydrogen is assumed to be the $\{N^{14}(n,p)C^{14}\}$ reaction of thermal neutrons with the nitrogen in the fuel. In these calculations it was assumed that all of the hydrogen produced by this reaction was absorbed by the T-111 fuel pin cladding. Although the calculated pickup of hydrogen is small, it exceeds the 1 to 2 ppm by weight which has been found to be sufficient to cause room temperature embrittlement of T-111 which has been aged at 990° C for long periods of time (1000 hr or more). All pins were essentially the same with regard to the amount of UN and T-111; so the calculation of hydrogen production was made only for one pin (table XII).

APPENDIX E

CALCULATION OF TOTAL STRAIN ON Cb-1Zr CLADDING FROM FISSION GASES RELEASED BY UO_2 FUEL IN 50 000 HOURS AT 990° C

The strain rate for the Cb-1Zr alloy at 982° C is (ref. 26)

$$\dot{\epsilon} = \left(\frac{\sigma}{1.062\times10^{8}}\right)^{4.83} \text{ cm/cm-hr} \tag{1}$$

The units of stress (σ) are newtons per square meter.

It is assumed for these calculations that the fission gas pressure and thus the cladding stress increase linearly with time. The instantaneous stress σ_i can then be expressed as a function of time t in hours:

$$\sigma_i = \frac{\sigma_F t}{5\times10^{4}} \tag{2}$$

where σ_F is the final cladding stress at 50 000 hours of irradiation time. The strain rate equation for Cb-1Zr becomes by combining equations (1) and (2)

$$\dot{\epsilon} = \left(\frac{\sigma_F t}{5.31\times10^{12}}\right)^{4.83} \tag{3}$$

To get the total strain ϵ_{total} over the 50 000 hours of irradiation this equation can be integrated as follows:

$$\epsilon_{total} = \int_0^{50\,000} \left(\frac{\sigma_F t}{5.31\times10^{12}}\right)^{4.83} dt = \left(\frac{\sigma_F}{5.31\times10^{12}}\right)^{4.83} \left[\frac{t^{5.83}}{5.83}\right]_0^{50\,000}$$

$$= 1.47\times10^{-35} \left(\sigma_F\right)^{4.83} \tag{4}$$

The stress on the cladding at the end of the irradiation is equal to the hoop stress:

$$\sigma_r = \frac{AD}{2l} \tag{5}$$

where σ_r is the final internal pressure of fission gases, D the inside diameter of the cladding, and l the wall thickness of the cladding.

For a reference design Cb-1Zr (95 percent dense UO_2) fuel pin with fission gas release after 50 000 hours equal to that of fuel pin 18, the values of D, l, and P_F are 0.016 meter, 0.00152 meter, and 16.63×10^5 newtons per square meter, respectively, at 990° C. The final stress on the cladding is then

$$\sigma_F = \frac{P_F D}{2l} = \frac{16.63\times10^5 \text{ N/m}^2 \times 1.6\times10^{-2} \text{ m}}{2 \times 1.52\times10^{-3} \text{ m}} = 8.75\times10^6 \text{ N/m}^2$$

Substituting the value for σ_F into equation (5) gives the total strain on the Cb-1Zr cladding at the end of 50 000 hours at an irradiation temperature of 990° C as

$$\epsilon_{total} = 1.47\times10^{-35} (8.75\times10^6)^{4.83} = 1.47\times10^{-35} \times 3.88\times10^{33} = 5.7\times10^{-2} = 5.7 \text{ percent}$$

REFERENCES

1. Krasner, Morton H.; Davison, Harry W.; and Diaguila, Anthony J.: Conceptual Design of a Compact Fast Reactor for Space Power. NASA TM X-67859, 1971.

2. Gluyas, R. E.; and Lietzke, A. F.: Materials Technology Program for a Compact Fast Reactor for Space Power. NASA TM X-67869, 1971.

3. Mayo, Wendall, Klann, Paul G.; and Whitmarsh, Charles L., Jr.: Nuclear Design and Experiments for a Space Power Reactor. NASA TM X-67857, 1971.

4. Gluyas, R. E.; and Watson, G. K.: Summary of Materials Program for an Advanced Space Power Reactor Concept. NASA TN D-7909, 1975.

5. Slaby, Jack G.; Siegel, Byron L.; Gedeon, Louis; and Galbo, Robert J.: Irradiation of Three T-111 (Ta-8W-2Hf) Clad Uranium Nitride Fuel Pins for 8070 Hours at 990° C (1815° F). NASA TM X-2878, 1973.

6. Slaby, Jack G.; Siegel, Byron L.; Bowles, Kenneth J.; and Galbo, Robert J.: Examination of T-111 Clad Uranium Nitride Fuel Pins Irradiated Up to 13 000 Hours at a Clad Temperature of 990° C. NASA TM X-2950, 1973.

7. Weinstein, Michael B.; Kirchgessner, Thomas A.; and Tambling, Thomas N.: Fission-Gas Release from Uranium Nitride at High Fission-Rate Density. NASA TN D-7171, 1973.

8. Thoms, K. R.: Design, Fabrication and Operation of Capsules for the Irradiation Testing of Candidate Advanced Space Reactor Fuel Pins. ORNL-TM-4825, Oak Ridge National Laboratory (NASA CR-134592), 1975.

9. DeCresente, M. A.; Freed, M. S.; and Caplow, S. D.: Uranium Nitride Fuel Development SNAP-50. PWAC-488, Pratt & Whitney Aircraft, 1965.

10. Weaver, S. C.; Scott, J. L.; Senn, R. L.; and Montgomery, B. H.: Effects of Irradiation on Uranium Nitride Under Space Reactor Conditions. ORNL-4461, Oak Ridge National Laboratories, 1969.

11. Cuneo, D. R.; Long, E. J., Jr.; Jostsons, A.; and Washburn, T. N.: Examination of Irradiated Uranium Nitride Fuel Clad with Tungsten-Rhenium or T-111 Alloy. ORNL-TM-3895, Oak Ridge National Laboratories, 1972.

12. Chubb, W.; Storhok, V. W.; and Keller, D. L.: Factors Affecting the Swelling of Nuclear Fuels at High Temperatures. Nuclear Tech., vol. 18, no. 3, June 1973, pp. 231-256.

13. Albrecht, E. D.; Rothman, A. J.; Lee, J. D.; Johnson, J. M.; and Hayes, W. N., Jr.: A High Temperature Irradiation and Post-Irradiation Analysis of Uranium Nitride Fuel. UCRL-50727, Lawrence Radiation Laboratory, 1969.

14. DeCarlo, V. A.; McQuilkin, F. R.; Senn, R. L.; Thoms, K. R.; and Weaver, S. C.: Design of a Capsule for Irradiation Testing of Uranium Nitride Fuel. ORNL-TM-2363, Oak Ridge National Laboratory, 1969.

15. Sinclair, John H.: Compatibility Tests of Materials for a Lithium-Cooled Space Power Reactor Concept. NASA TN D-7259, 1973.

16. Frank, R. G.; Miketta, D. N.; Kearns, W. H.; Young, W. R.; and Hand, R. B.: Materials and Process Specifications for Refractory Alloy and Alkali Metals. R66SD3007, General Electric Co. (NASA CR-88711), 1965.

17. Tennery, V. J.; Godfrey, T. G.; and Potter, R. A.: Synthesis, Characterization, and Fabrication of UN. ORNL-4608, Oak Ridge National Laboratory (NASA CR-72764), 1970.

18. Moore, T. J.; Moorhead, P. E.; and Bowles, K. J.: Specifications for Cleaning, Fusion Welding, and Postheating Tantalum and Columbium Alloys. NASA TM X-67879, 1971.

19. Foster, B. W.; Snyder, S. D.; DeCarlo, V. A.; and McClung, R. W.: Development and Operation of a High-Intensity, High-Resolution Neutron Radiograph Facility. ORNL-4738, Oak Ridge National Laboratory, 1971.

20. Vary, Alex; and Bowles, Kenneth J.: Application of an Electronic Image Analyzer to Dimensional Measurements from Neutron Radiographs. NASA TM X-68200, 1973.

21. Watson, Gordon K.; and Stephens, Joseph R.: Effect of Aging at 1040° C (1900° F) on the Ductility and Structure of a Tantalum Alloy, T-111. NASA TN D-6988, 1972.

22. Davison, Harry W.; and Fiero, Ivan B.: Calculation of Radiation Induced Swelling of Uranium Mononitride Using the Digital Computer Program CYGRO2. NASA TM X-2224, 1971.

23. Liu, C. T.; Inouye, H.; and Carpenter, R. W.: Mechanical Properties and Structure of Oxygen-Doped Tantalum Base Alloy. ORNL-4839, Oak Ridge National Laboratory, 1973.

24. Buzzard, Robert J.; and Metroka, Robert R.: Effect of Nitrogen on Tensile Properties and Structures of T-111 (Tantalum, 8 Percent Tungsten, 2 Percent Hafnium) Tubing. NASA TN D-6999, 1973.

25. Gahn, Randall F.: Effects of Low-Pressure Air on Oxygen Contamination and Lithium Corrosion Reactions of a Tantalum Alloy, T-111 at 980° and 1260° C. NASA TN D-7588, 1974.

26. Gedeon, Louis; and Lietzke, Armin F.: Analysis of Cylindrical Reactor Fuel Pin for Clad Stress Caused by Fission Gases. NASA TN D-5178, 1969.

27. Tipton, C. R. Jr., ed.: Reactor Handbook. Second ed., Interscience Publishers, Inc., 1960, pg. 990.

TABLE I. - PINS USED IN IRRADIATION CAPSULES

(a) Capsule UN-4

	Fuel pin		
	10	11	12
Position in capsule	Top pin	Middle pin	Bottom pin
Cladding material	T-111	T-111	T-111
Cladding liner material	Tungsten	Tungsten	Tungsten
Fuel pellets:			
Material	UN	UN	UN
^{235}U enrichment, percent	19.86	10.96	10.96
Density, percent theoretical	85.82 to 86.03	83.94 to 84.78	93.85 to 94.27
Stack length, cm	7.62229	7.62457	7.61721
Weight, g	44.9204	44.0493	44.9044
Outside diameter, cm	0.7803 to 0.7823	0.7800 to 0.7816	0.7803 to 0.7818
Inside diameter, cm	----------	----------	0.2273 to 0.2299
Number of pellets	8	9	8

(b) Capsule UN-5

	Fuel pin		
	13	14	15
Position in capsule	Top pin	Middle pin	Bottom pin
Cladding material	T-111	T-111	T-111
Cladding liner material	Tungsten	Tungsten	Tungsten
Fuel pellets:			
Material	UN	UN	UN
^{235}U enrichment, percent	19.86	10.96	10.96
Density, percent theoretical	85.54 to 86.73	93.85 to 94.28	83.94 to 84.78
Stack length, cm	7.61949	7.62203	7.62051
Weight, g	44.9513	44.9927	44.0773
Outside diameter, cm	0.7798 to 0.7823	0.7810 to 0.7816	0.7803 to 0.7818
Inside diameter, cm	----------	0.2261 to 0.2299	----------
Number of pellets	8	8	9

(c) Capsule UN-6

	Fuel pin		
	16	17	18
Position in capsule	Top pin	Middle pin	Bottom pin
Cladding material	Cb-1Zr	T-111	Cb-1Zr
Cladding liner material	Tungsten	Tungsten	Tungsten
Fuel pellets:			
Material	UO_2	UO_2	UO_2
^{235}U enrichment, percent	10	10	8
Density, percent theoretical	95.26 to 95.62	95.26 to 95.44	95.80 to 96.08
Stack length, cm	7.6200	7.62406	7.62229
Weight, g	35.475	35.478	35.647
Outside diameter, cm	0.7823	0.7823	0.7823
Inside diameter, cm	0.213	0.213	0.213
Number of pellets	10	10	10

TABLE II. - DESCRIPTION OF FUEL PINS FOR THERMAL SIMULATION TESTS

	Fuel pin							
	S-2	S-3	S-7	S-8	S-9	S-6	S-17	S-18
	Simulates fuel pin -							
	10 and 13	10 and 13	11 and 15	12 and 14	12 and 14	16	17	18
Cladding material	T-111	T-111	T-111	T-111	T-111	Cb-1Zr	T-111	Cb-1Zr
Cladding liner material	Tungsten	Tungsten	Tungsten	Tungsten	Tungsten	Tungsten	Tungsten	Tungsten
Fuel pellets:								
Material	UN	UN	UN	UN	UN	UO_2	UO_2	UO_2
^{235}U enrichment, percent	19.86	19.86	10.96	10.96	10.96	10	10	8
Density, percent theoretical	84.92 to 86.38	84.85 to 85.61	84.08 to 84.78	93.79 to 94.34	93.99 to 94.41	95.07 to 95.53	95.16 to 95.80	95.62 to 96.08
Stack length, cm	7.6220	7.6187	7.6233	7.6205	7.6213	7.6225	7.6187	7.6225
Weight, g	44.7361	44.5592	44.0732	45.0132	45.0822	35.474	35.462	35.649
Outside diameter, cm	0.7803 to 0.7823	0.7803 to 0.7818	0.7798 to 0.7811	0.7800 to 0.7818	0.7798 to 0.7818	0.7823	0.7823	0.7823
Inside diameter, cm	----------	----------	----------	0.226 to 0.2286	0.2261 to 0.2299	0.213	0.213	0.213
Number of pellets	8	8	9	8	8	10	10	10

TABLE III. - ISOTOPIC AND CHEMICAL ANALYSIS OF UN PELLETS USED IN UN-4, UN-5, AND THERMAL SIMULATION PINS

	Fuel pin		
	S-2, S-3, 10, and 11	S-8, S-9, 12, and 14	11, 15, S-7
^{233}U (wt. %)	<0.0005	<0.0005	<0.0005
^{234}U (wt. %)	0.131	0.099	0.090
^{235}U (wt. %)	19.86	10.96	10.96
^{236}U (wt. %)	0.122	0.043	0.043
^{238}U (wt. %)	79.89	79.89	88.90
N (wt. %)	5.38 to 5.37	5.41 to 5.46	5.49 to 5.48
U (wt. %)	94.40 to 94.41	94.41 to 94.42	94.36 to 94.34
O (ppm)	1000, 1230, 1260	1050, 1070	1270, 1330
C (ppm)	330, 330	280, 380	120, 170
B (ppm)	0.4	1	0.4

TABLE IV. - ISOTOPIC AND CHEMICAL ANALYSIS OF UO_2 PELLETS USED IN UN-6 AND THERMAL SIMULATION PINS

[O/U ratio: for fuel pins 17 and S-17, 2.003; for fuel pins 16, 18, S-16, and S-18, 2.005.]

	Fuel pin	
	17 and S-17	16, 18, S-16, and S-18
^{233}U (wt. %)	<0.0005	<0.001
^{234}U (wt. %)	.059	.075
^{235}U (wt. %)	8.27	10.28
^{236}U (wt. %)	.031	.040
^{238}U (wt. %)	91.64	89.60

TABLE V. - LEAK TEST RESULTS AND WEIGHT CHANGES ON IRRADIATED FUEL PINS

Fuel pin	Cladding	Fuel	Leak indication (helium mass spectrometer)	Preirradiated weight, g	Postirradiated[a] corrected weight, g	Weight change, g
10	T-111	85 Percent dense UN	Very slight leak indicated	102.444	102.516	+0.072
11		85 Percent dense UN	No leak indicated	100.705	100.692	-.013
12		95 Percent dense UN	Cracked; not tested	103.286	104.592	+1.306
13		85 Percent dense UN	No leak indicated	102.862	102.816	-.046
14		95 Percent dense UN	Cracked; not tested	102.488	105.437	+3.051
15		85 Percent dense UN	Slight leak indicated	102.780	102.757	-.023
16	Cb-1Zr	95 Percent dense UO_2	Very slight leak indicated	69.453	69.547	+.094
17	T-111	95 Percent dense UO_2	No leak indicated	93.455	93.444	-.011
18	Cb-1Zr	95 Percent dense UO_2	No leak indicated	70.307	70.309	+.002

[a]Solid fuel pin extension broke off inside cup extension on pin below when pins were removed from NaK capsule. Weight differential caused by this equal to 0.2 to 0.3 g. Tungsten wire tying extension cups to extension rods included in postirradiation weights.

TABLE VI. - FISSION GAS RELEASE FROM FUEL

Fuel pin	Cladding	Fuel	Pressure in void, N/m^2	Percent fission gas release (calculated)
11	T-111	85 Percent dense UN	2.70×10^5	4.3
17	T-111	95 Percent dense UO_2	4.55×10^5	34.9
18	Cb-1Zr	95 Percent dense UO_2	3.95×10^5	26.4

TABLE VII. - FUEL BURNUP VALUES FOR SELECTED FUEL PINS

Fuel pin	Cladding	Fuel	Averaged fuel burnup values, percent	
			Calculated from calorimeter data	Measured by gamma scan and isotopic analysis
11	T-111	85 Percent dense UN	2.83	2.76
14	T-111	95 Percent dense UN	2.64	3.11
17	T-111	95 Percent dense UO_2	1.76	2.28
18	Cb-1Zr	95 Percent dense UO_2	2.04	1.95

TABLE VIII. - CLADDING DIAMETRAL STRAIN TEST RESULTS

Fuel pin	Cladding	Fuel	Cladding ring expansion ductility, percent	
			As-irradiated	After 1040° C, 1 hr anneal
11	T-111	85 Percent dense UN	1.0	>6.0
14	T-111	95 Percent dense UN	Brittle[a]	Ductile[b]
17	T-111	95 Percent dense UO_2	1.0	Brittle[c]
18	Cb-1Zr	95 Percent dense UO_2	>7.0	>8.0

[a]Cracked during irradiation.

[b]Determined by flattening in a vise not by ring expansion.

[c]Amount of expansion not measured; ductility not improved over as-irradiated measurement.

TABLE IX. - UN FUEL PELLET DENSITIES

Fuel pin	Preirradiation density, percent true density	Postirradiation density	
		Calculated density, percent theoretical density	CCl immersion density, percent theoretical density
11	84.8	80.2	86.3
14	94.3	76.5	80.6

TABLE X. - INTERSTITIAL ANALYSIS OF CLADDING MATERIAL FROM THERMAL SIMULATION FUEL PINS

Fuel pin	Cladding	Fuel	Pretest, ppm by weight			Posttest, ppm by weight		
			O^a	N^a	H^b	O^c	N^c	H^b
S-7	T-111	85 Percent dense UN	48	18	<1	49	35	0.7
S-8	T-111	95 Percent dense UN	48	18	<1	68	36	1.6
S-17	T-111	95 Percent dense UO_2	23	8	<1	68	20	1.3
S-18	Cb-1Zr	95 Percent dense UO_2	26	8	12	230	23	2.3

[a]Vacuum fusion analysis; ±1 ppm by weight.

[b]Vacuum fusion analysis; ±0.5 ppm by weight.

[c]Inert gas fusion analysis; ±0.5 percent of listed value.

TABLE XI. - MAXIMUM FUEL PIN DIAMETRAL SWELLING

Fuel pin	Cladding	Fuel	Irradiation time, hr	Fuel burnup, metal at. %		Cladding diametral change, (ΔD 0)100, percent
				Measured[a]	Calculated	
[b]10	T-111	85 Percent dense UN	10 450	(c)	2.87	0.2
11		85 Percent dense UN	10 450	2.76	2.83	.3
[b]12		95 Percent dense UN	10 450	(c)	2.74	[d]1.5
[b]13		85 Percent dense UN	10 035	(c)	2.79	.2
14		95 Percent dense UN	10 035	3.11	2.64	[d, c]3.7
[b]15		85 Percent dense UN	10 035	(c)	2.72	.4
[b]16	Cb-1Zr	95 Percent dense UO_2	8 333	(c)	1.67	.5
17	T-111	95 Percent dense UO_2	8 333	2.28	1.76	.5
18	Cb-1Zr	95 Percent dense UO_2	8 333	1.95	2.04	1.0

[a]Isotopic analysis.

[b]Not tested; sent to ORNL.

[c]Not done.

[d]Cracked.

[e]Measurement of axial bulge of cladding directly opposite the crack indicates cladding strain was 1.5 percent when cladding cracked.

TABLE XII. - SAMPLE CALCULATION OF HYDROGEN FROM $\left\{N^{14}(n,p)C^{14}\right\}$ REACTION IN UN FUEL

[Outer diameter of fuel, D_o, cm; inner diameter of fuel, D_i, cm; Avogadro's number, N_A; molecular weight, MW.]

Item	Fuel pin 14 (95 percent dense UN)
Volume of fuel cylinders, $V_f = \pi/4\left(D_o^2 - D_i^2\right)$, cm^3	3.33
Flux[a], φ, neutrons/cm^2-sec	2×10^{13}
Irradiation time[a], t, sec	3.6×10^{7}
Reaction cross section[b] (E = 0.025 eV), $\sigma(n,p)$, b	1.9
Fuel density[c], ρ, g/cm^3	13.5
Molecules of UN/cm^3, $\rho N_A/MW$	3.27×10^{22}
Total nitrogen reaction cross section, $\sum(n,p) = \sigma(n,p) \times$ molecules of UN/cm^3, cm^{-1}	6.21×10^{-2}
Reaction rate density, $K_R = \sum(n,p)\varphi$	12.4×10^{11}
Number of protons generated, $N_p = V_f K_R t$	1.49×10^{20}
Moles of hydrogen, $M_{H_2} = N_P/2N_A$	1.23×10^{-4}
Weight of hydrogen, $W_{H_2} = M_{H_2} MW_{H_2}$	2.46×10^{-4}
Weight of T-111[a], $W_{T\text{-}111}$, g	48.9
End of life concentration of hydrogen in T-111, $\left[W_{H_2}/\left(W_{T\text{-}111} + W_{H_2}\right)\right]10^6$, ppm by weight	5.0

[a]Measured.

[b]Ref. 27.

[c]From measured weight and dimensions.

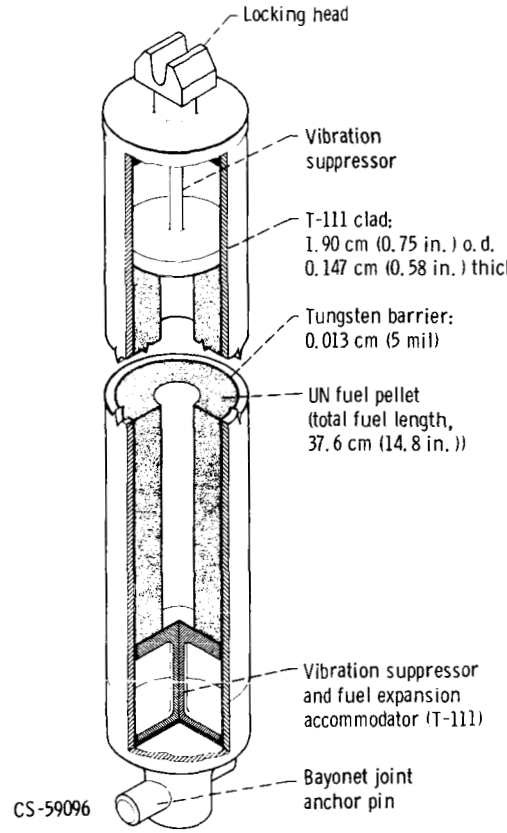

Figure 1. - Advanced power reactor concept fuel pin.

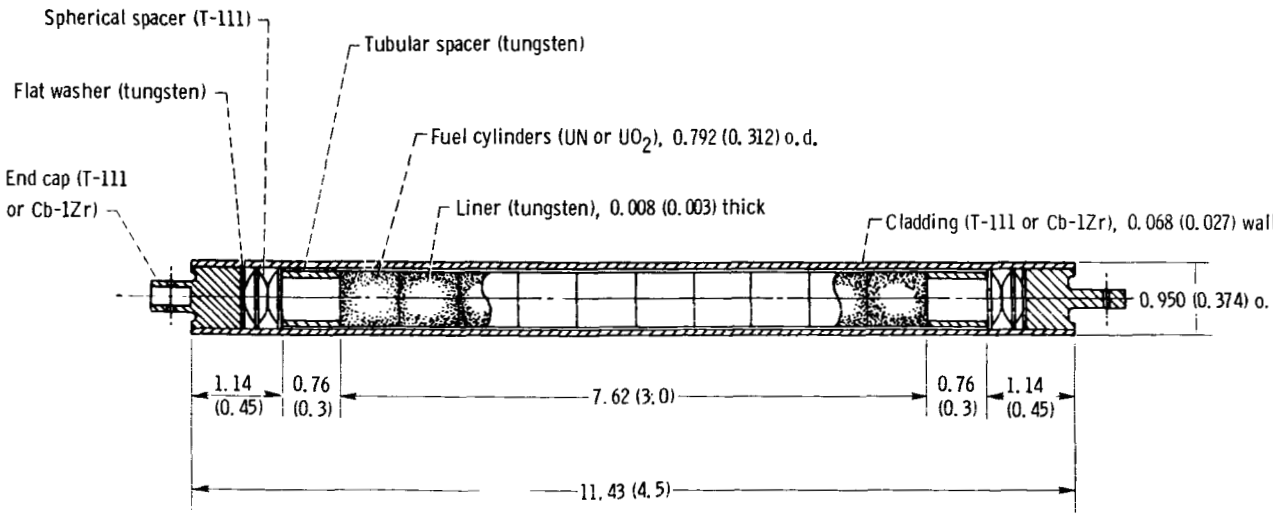

Figure 2. - Typical test fuel pin configuration. All dimensions are in centimeters (in.).

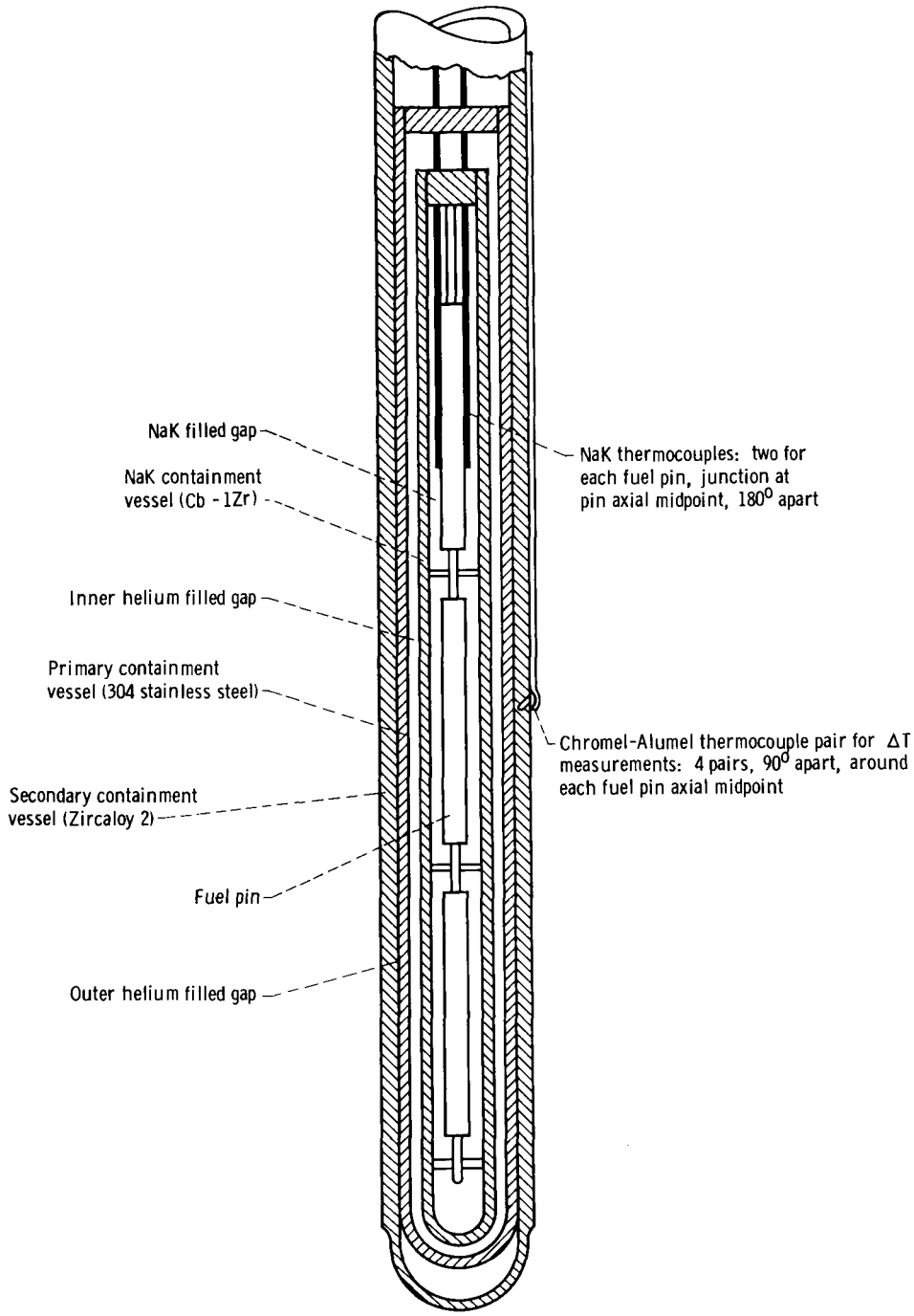

Figure 4. - Fuel pin irradiation capsule configuration.

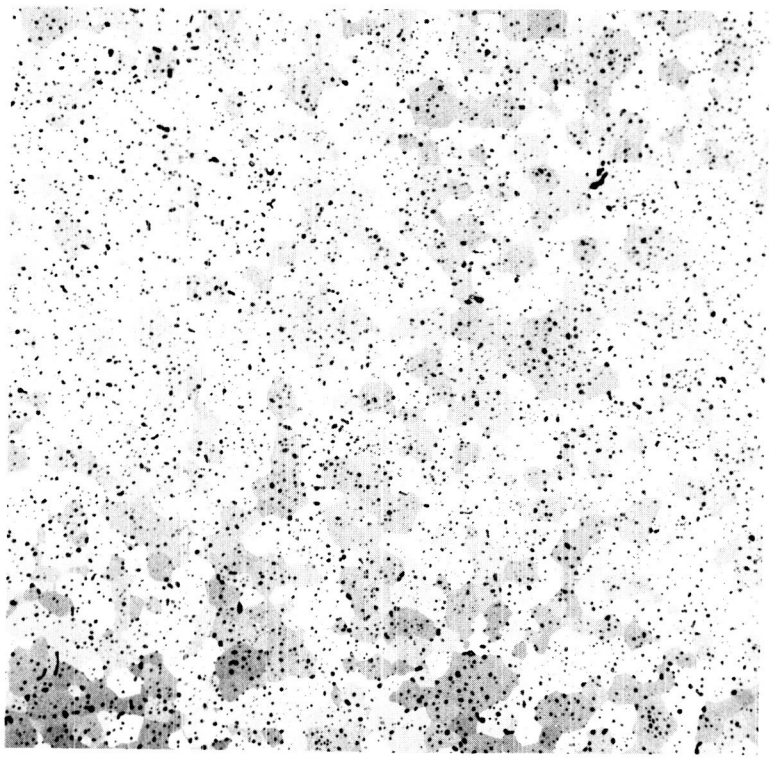

(a) Magnification, 100.

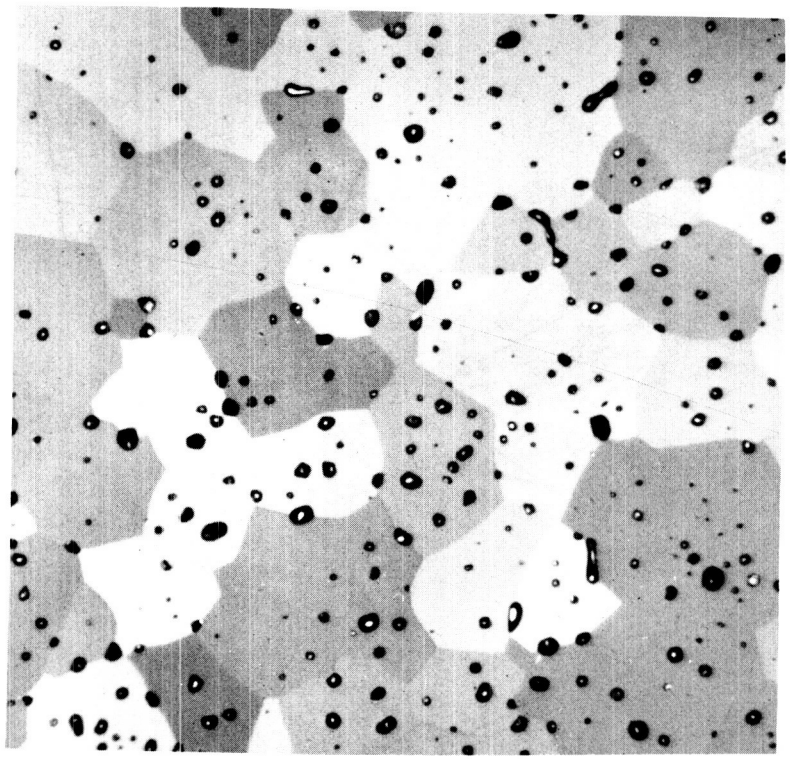

(b) Magnification, 500.

Figure 5. - Typical microstructure of uranium mononitride in etched condition. Etchant: 60 milliliters lactic acid, 24 milliliters nitric acid, 2 milliliters hydrofluoric acid.

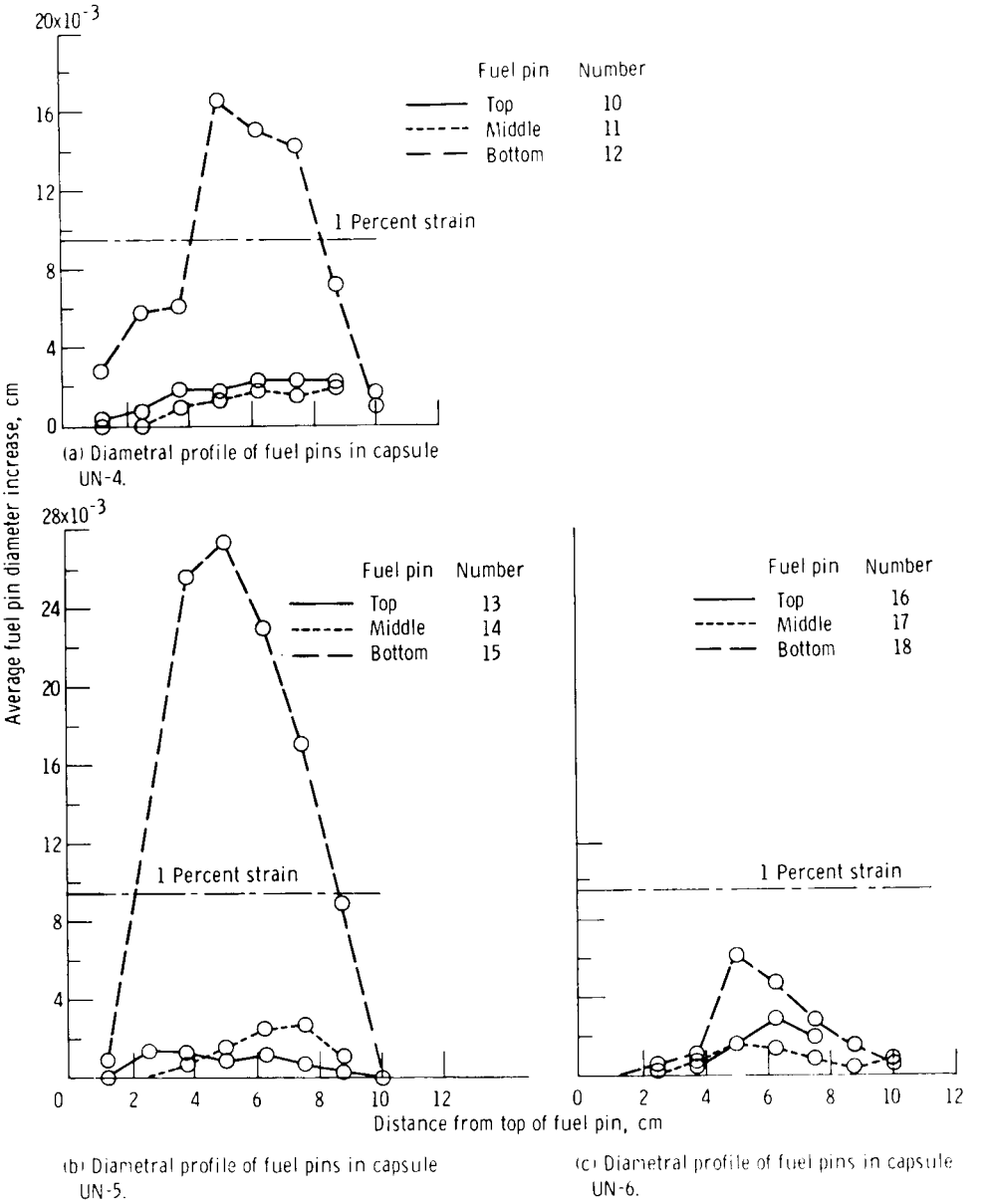

(a) Diametral profile of fuel pins in capsule UN-4.

(b) Diametral profile of fuel pins in capsule UN-5.

(c) Diametral profile of fuel pins in capsule UN-6.

Figure 6. - Fuel pin diametral changes after irradiation.

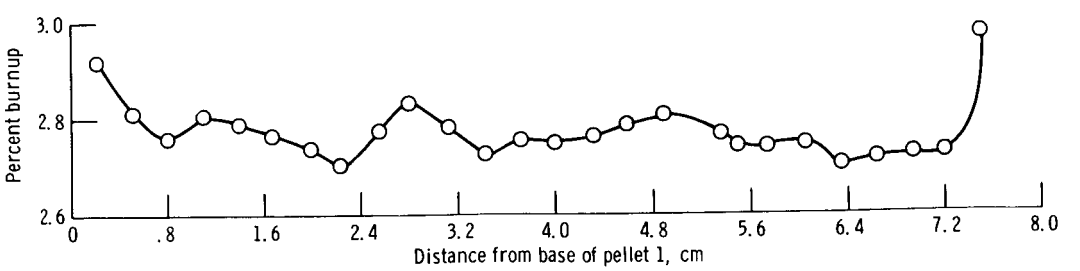

Figure 7. - Measured burnup profile in pin 11 (T-111 and 85 percent dense UN) from gamma scan normalized by isotopic mass spectrometer analysis.

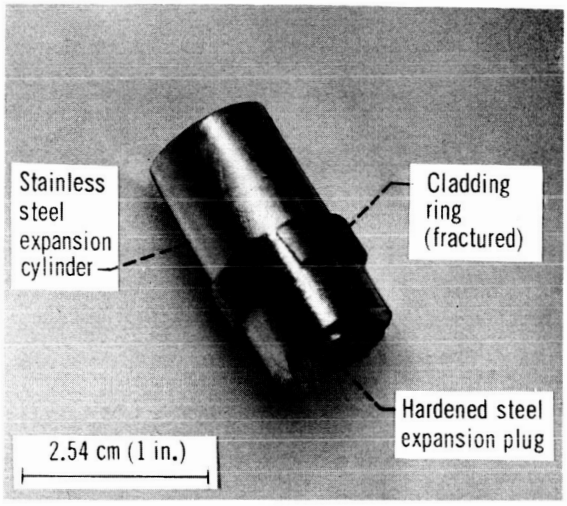

Figure 8. - Ductility ring expansion test components.

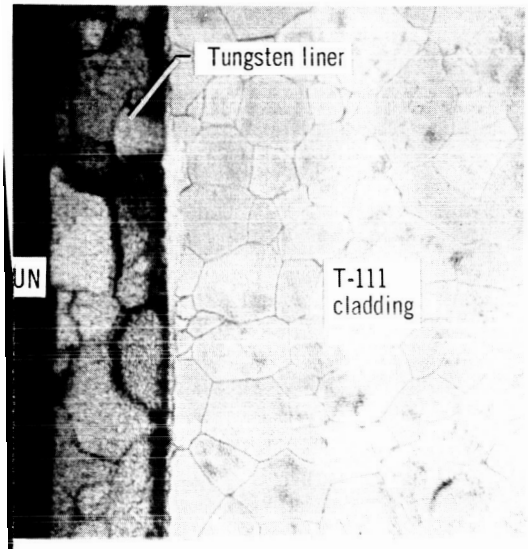

(a) Pin 14. 95-Percent dense UN; 10 035 hours at 990° C; etched. ×250.

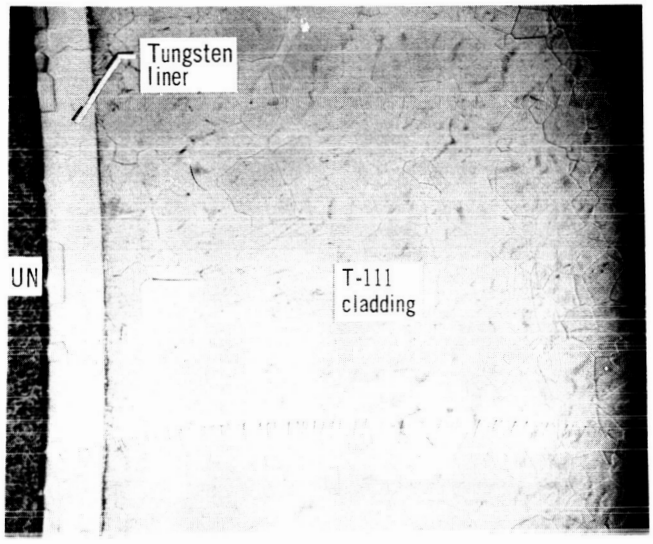

(b) Pin 11. 85-Percent dense UN; 10 045 hours at 990° C; etched. ×125.

Figure 9. - Microstructure of irradiated T-111 cladding and tungsten liner from UN fueled pins.

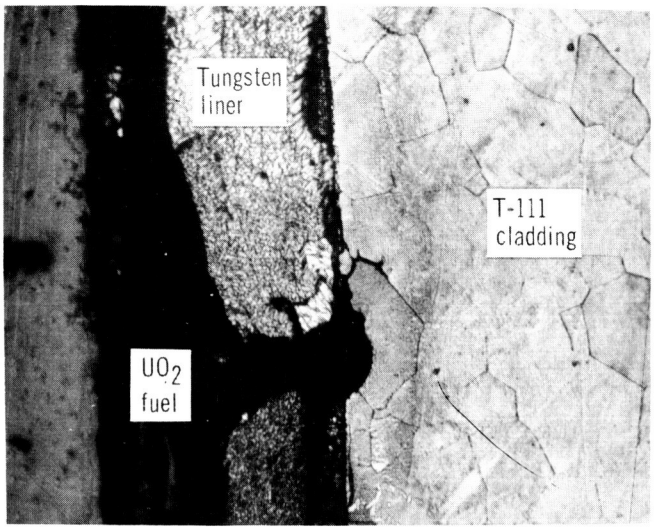

Figure 10. - Irradiated T-111 cladding (8333 hr at 990° C) from 95 percent dense UO_2 fuel pin. Note erosion and grain boundary separation in T-111 at liner crack. Etched. ×250.

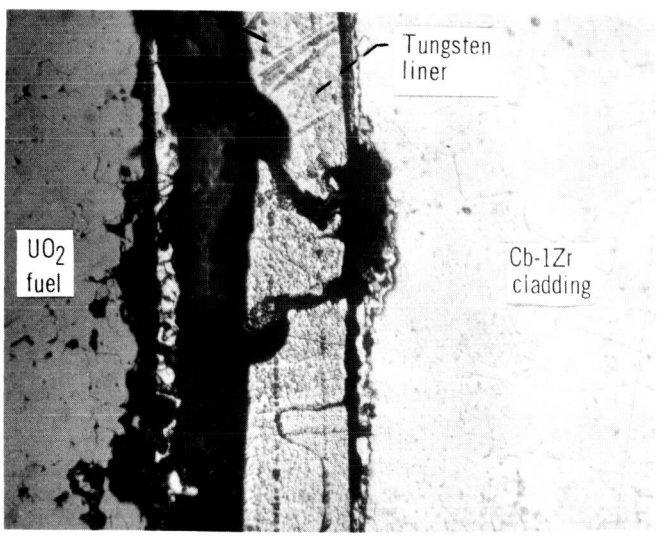

Figure 11. - Irradiated Cb-1Zr cladding (8333 hr at 990° C) from 95 percent dense UO_2 fuel pin. Note erosion in cladding at liner crack. Etched. ×250.

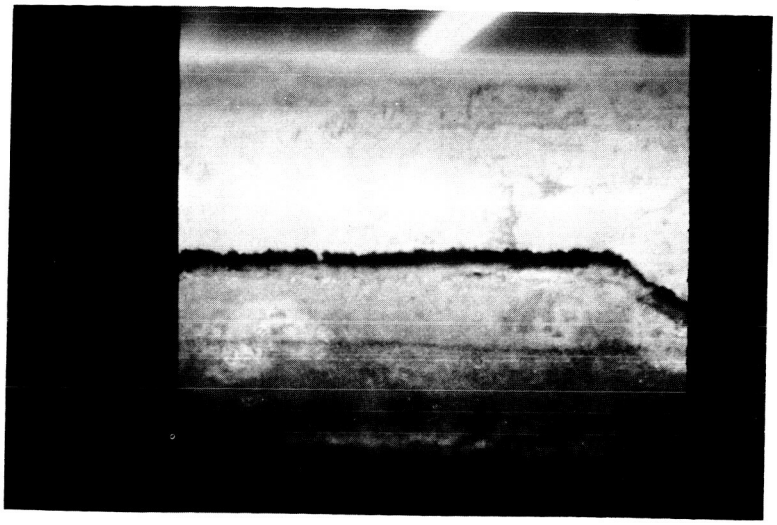

Figure 12. - Crack in T-111 cladding of 95 percent dense UN fuel pin 14. Crack width, ≈ 0.053 centimeter (0.021 in.). Fuel pin irradiated for 10 035 hours at 990° C. ×6.

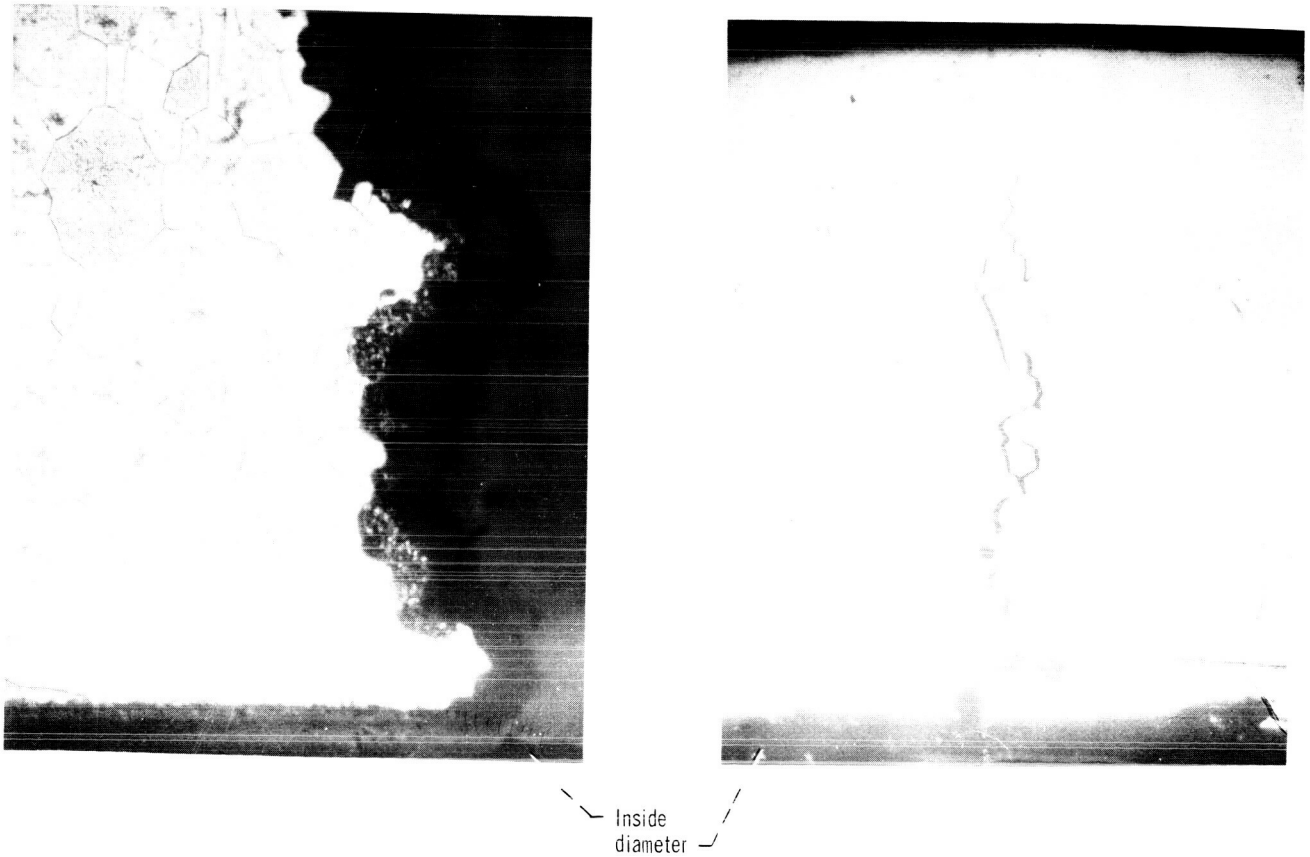

(a) Crack edge in T-111 cladding. Etched.

(b) T-111 cladding crack, 95 percent dense UN fuel pin. Unetched.

Figure 13. - Cladding cracks in T-111 and 95 percent dense UN irradiated for 10 035 hours at 990° C. ×250.

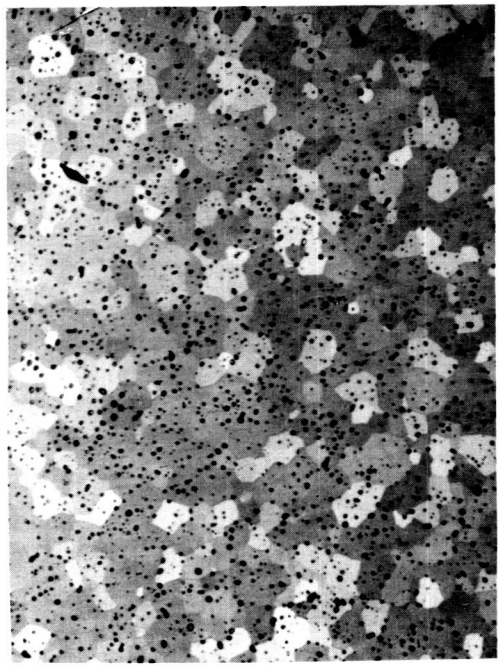

(a) 95-Percent dense UN.

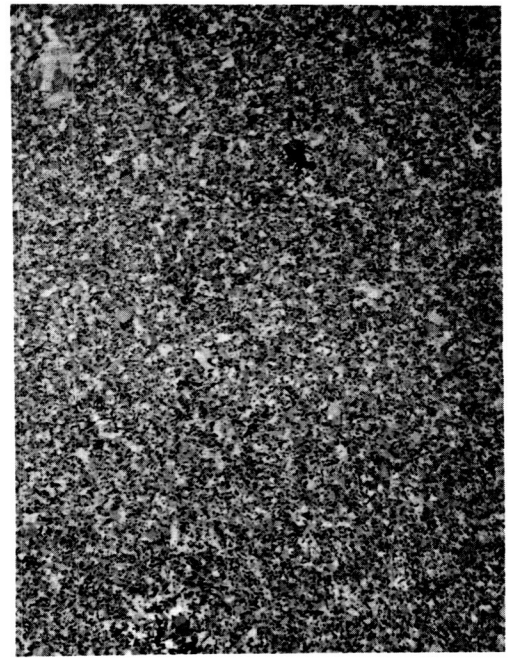

(b) 85-Percent dense UN.

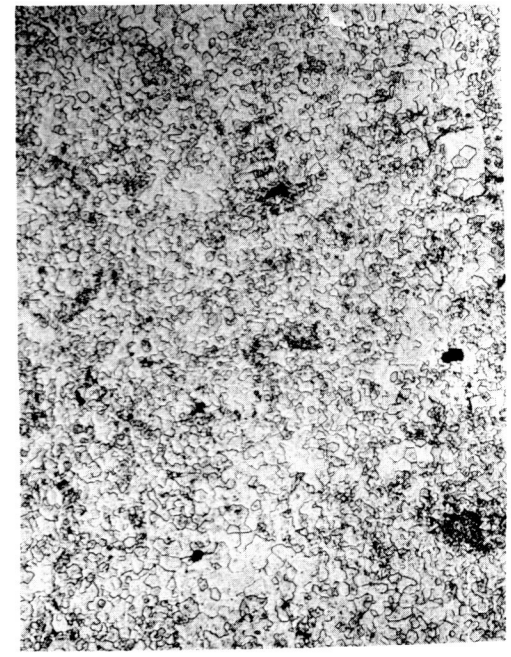

(c) 95-Percent dense UO_2.

Figure 14. - Thermally aged UN and UO_2 fuel (unirradiated). Etched. ×250.

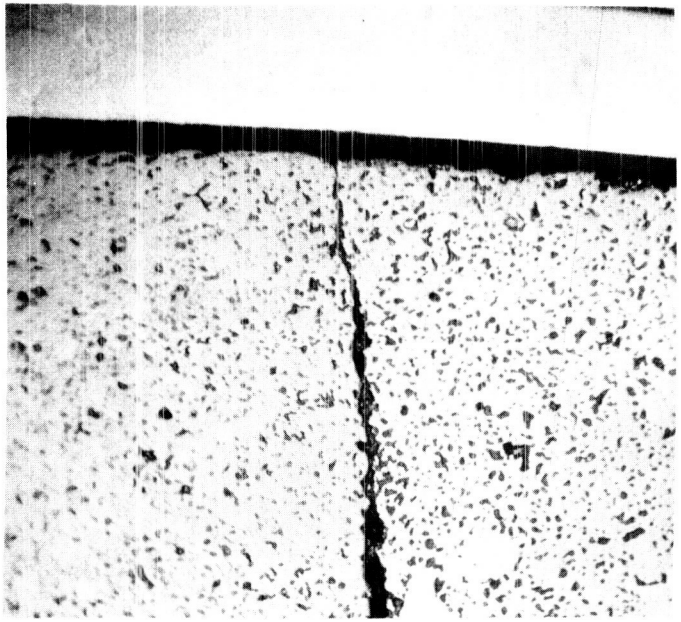

Figure 15. - Irradiated 85 percent dense UN fuel (10 450 hr at 990° C). Unetched. ×250.

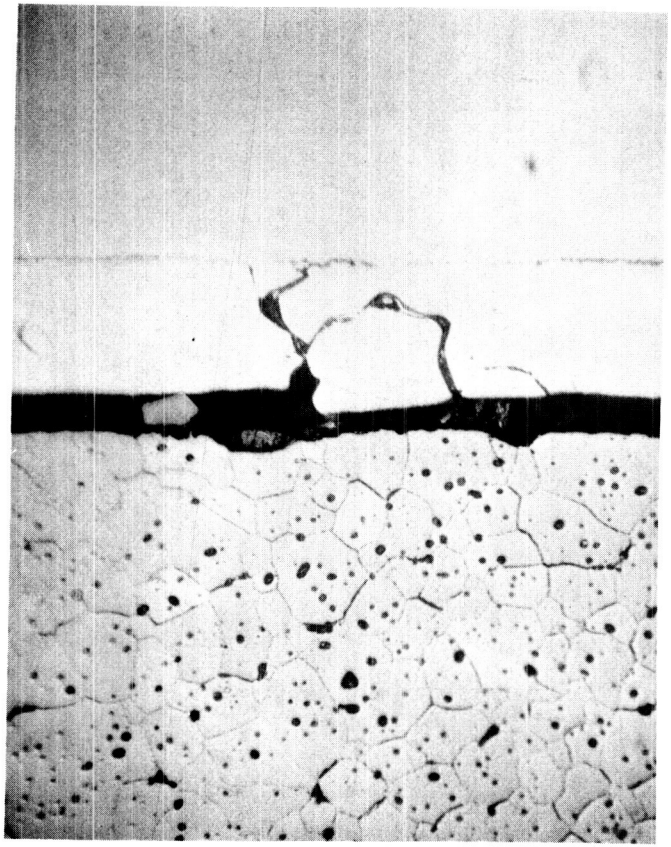

Figure 16. - Irradiated 95 percent dense UN fuel showing voids in grain boundaries. Unetched. ×250.

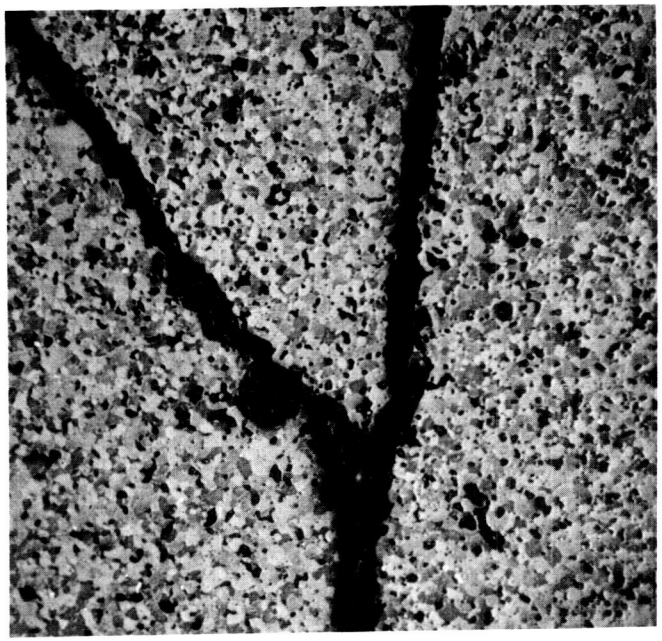

Figure 17. - Irradiated 85 percent dense UN fuel (10 450 hr at 990° C). Note small white second-phase particles. Etched. ×250.

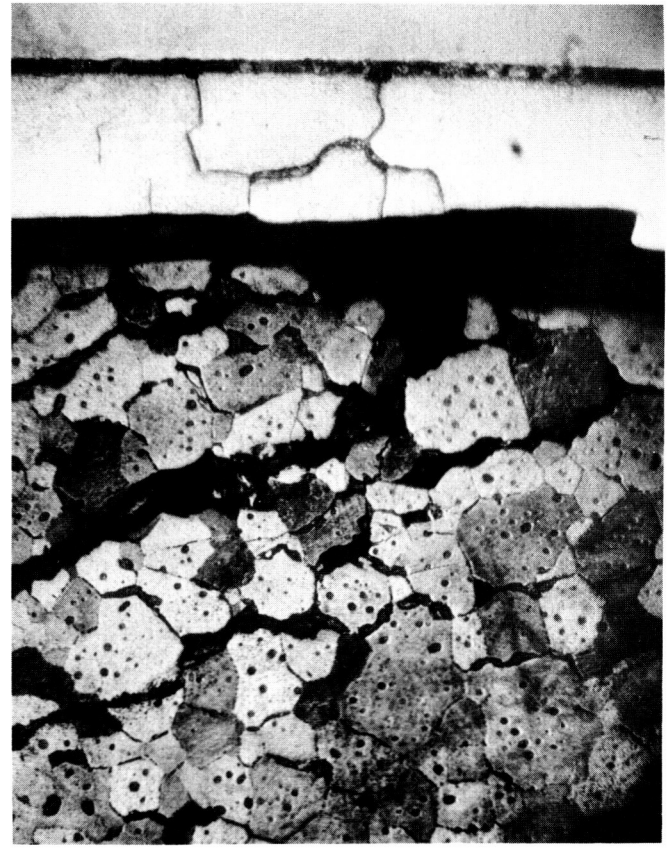

Figure 18. - Irradiated 95 percent dense UN fuel (10 035 hr at 990° C). No second phase is visible; note separation of grains. Etched. ×250.

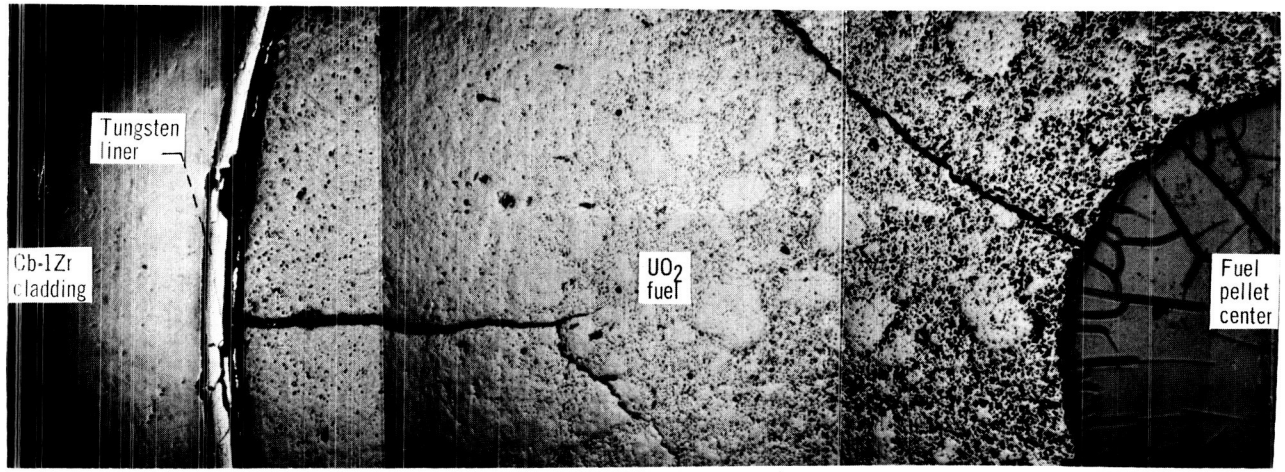

Figure 19. - UO_2 fuel from pin 18 (833 hr at 990° C). Note high number or voids near center of pellet and small depressions in inner surface of cladding at liner cracks. Unetched. ×50.

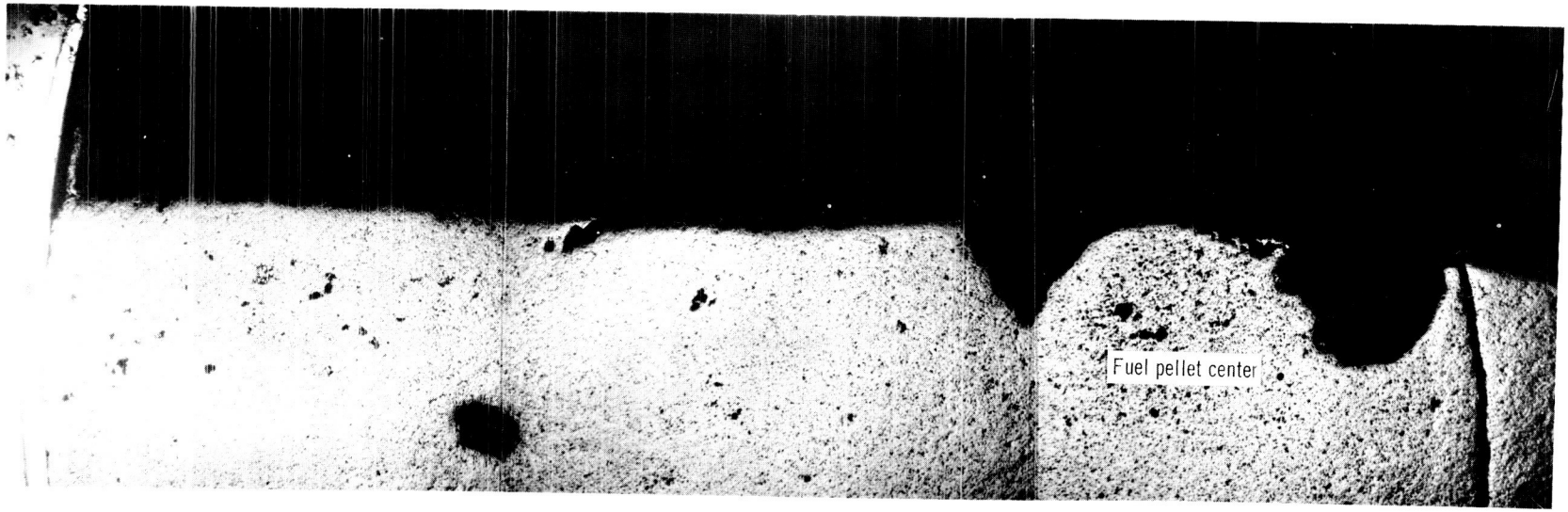

Figure 20. - Diametral section of 85 percent dense UN fuel. Irradiated 10 450 hours at 990° C. Note even distribution of voids. Unetched. ×50.

(a) T-111 and 85 percent dense UN.

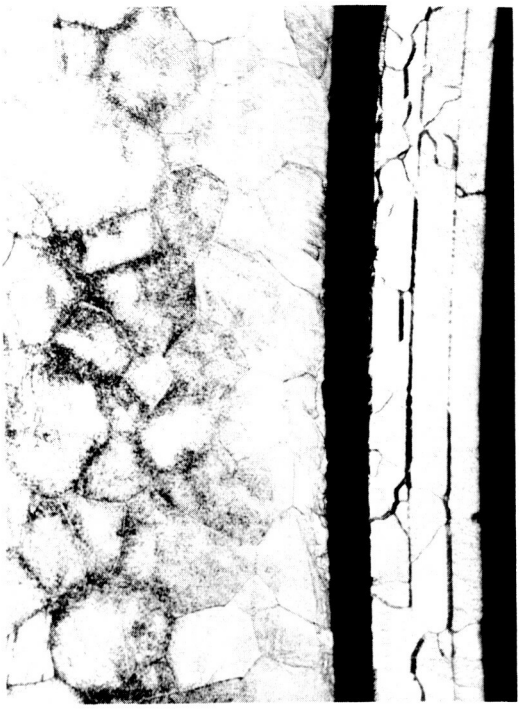

(b) T-111 and 95 percent dense UN.

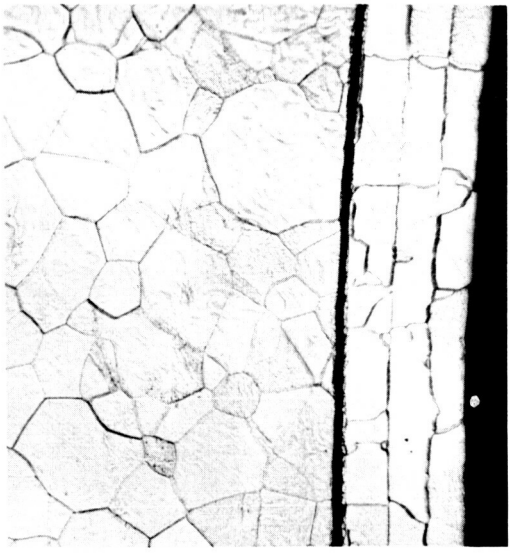

(c) T-111 and 94 percent dense UO_2.

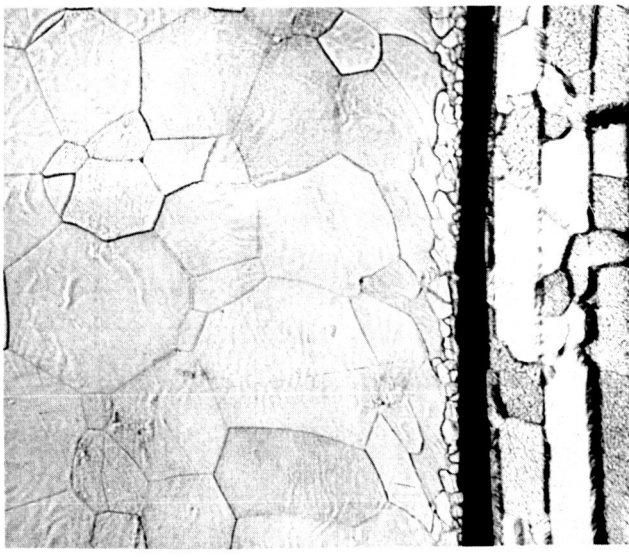

(d) Cb-1Zr and 94 percent dense UO_2.

Figure 21. - Microstructure of out-of-reactor thermal simulation pin claddings. Etched. ×250.